LA-UR-23-25949
Accepted Manuscript

Recent Developments in Sensor Technologies for Enabling the Hydrogen Economy

Brosha, Eric Lanich; Ramaiyan, Kannan; Tsui, Lok-kun; Stetter, Joseph R.; Russ, Tamara; Du, Winncy; Peaslee, David; Hunter, Gary; Xu, Jennifer; Makel, Darby; Garzon, Fernando H.; Mukundan, Rangachary

To be published in: ECS Sensors Plus

DOI to publisher's version: 10.1149/2754-2726/ad0736

Permalink to record:
https://permalink.lanl.gov/object/view?what=info:lanl-repo/lareport/LA-UR-23-25949

Recent Developments in Sensor Technologies for Enabling the Hydrogen Economy

ECS Sensors Plus, 2023 **2** 045601

Recent Developments in Sensor Technologies for Enabling the Hydrogen Economy

Kannan Ramaiyan,[1,*,z] Lok-kun Tsui,[1] Eric L. Brosha,[2] Cortney Kreller,[2,*] Joseph R. Stetter,[3,] Tamara Russ,[3,4] Winncy Du,[4] David Peaslee,[3] Gary Hunter,[5] Jennifer Xu,[5] Darby Makel,[6] Fernando Garzon,[1,**] and Rangachary Mukundan[7,**,z]**

[1]*Center for Micro-Engineered Materials, University of New Mexico, Albuquerque, New Mexico 87106, United States of America*
[2]*MPA-11, Los Alamos National Laboratory, Los Alamos, New Mexico, United States of America*
[3]*Interlink Electronics Inc., 94560 Newark, California, United States of America*
[4]*San Jose State University, Mechanical Engineering Department, Robotics, Sensors and Machine Intelligence Lab, 95192 San Jose, California, United States of America*
[5]*NASA Glenn Research Center, Cleveland, Ohio, United States of America*
[6]*Makel Engineering Inc. Chico, California, United States of America*
[7]*Lawrence Berkeley National Laboratory, California, United States of America*

Efforts to create a sustainable hydrogen economy are gaining momentum as governments all over the world are investing in hydrogen production, storage, distribution, and delivery technologies to develop a hydrogen infrastructure. This involves transporting hydrogen in gaseous or liquid form or using carrier gases such as methane, ammonia, or mixtures of methane and hydrogen. Hydrogen is a colorless, odorless gas and can easily leak into the atmosphere leading to economic loss and safety concerns. Therefore, deployment of robust low-cost sensors for various scenarios involving hydrogen is of paramount importance. Here, we review some recent developments in hydrogen sensors for applications such as leak detection, safety, process monitoring in production, transport and use scenarios. The status of methane and ammonia sensors is covered due to their important role in hydrogen production and transportation using existing natural gas and ammonia infrastructure. This review further provides an overview of existing commercial hydrogen sensors and also addresses the potential for hydrogen as an interferent gas for currently used sensors. This review can help developers and users make informed decisions about how to drive hydrogen sensor technology forward and to incorporate hydrogen sensors into the various hydrogen deployment projects in the coming decade.
 [DOI: 10.1149/2754-2726/ad0736]

Manuscript submitted June 23, 2023; revised manuscript received September 27, 2023. Published December 12, 2023.

The hydrogen economy has been envisioned as a low-pollution alternative to the fossil fuel economy ever since the first article on this topic was published in 1972.[1,2] After 50 years and many false starts later, the hydrogen economy seems to have turned a corner with renewed interest. In this new hydrogen economy scenario, hydrogen is expected to play a key role in the energy and transportation sectors, the building sector as heat source, the power sector as seasonal renewable energy, and significantly expand its current utility in areas such as the industrial sector as a chemical feedstock. Hydrogen is heavily used in chemical production and oil refineries that accounts for more than 90% of its current consumption. At the moment its contributions towards the transportation and energy storage sectors are minimal, however, it is expected to grow multifold over the coming decade in part as a response to climate change. Many countries have started to invest in hydrogen technologies as a means to meet the goals set by the Conference of Parties 21 (COP21). Recently, the United States has increased its investment in hydrogen with $9.5 Billion available for clean hydrogen initiatives in the Bipartisan Infrastructure Law (BIL).[3] As a result of these investments from multiple governments, many new initiatives are being formed to utilize hydrogen, especially in the transportation sector. One of these initiatives is called Hysetco, a partnership between four companies intending to use 600 hydrogen fuel cell vehicles (Toyota Mirai) as *t*axis for commuting in Paris.[4] There are fourteen Alstom Coradia iLint hydrogen-powered passenger trains currently in use in Germany between Cuxhaven, Bremervörde and Buxtehude with a single fueling station, the Linde facility in Bremervörde.[5] Moreover, the global sales of fuel cell vehicles like the Hyundai Nexo and the Toyota Mirai exceeded 15,000 cars in 2021. These trends clearly indicate that the use of hydrogen for transportation is already on the rise despite the limited infrastructure. In 2020, the demand for hydrogen was at about 90 million tons (Mt) that were primarily utilized in three sectors: refineries, chemical production and steel making. The demand is projected to increase significantly, especially in the transportation and power sectors with governments across the globe pledging net zero emissions by 2050 which requires the production of 530 Mt of H_2.[6]

Nearly all of the current hydrogen demand is met by fossil fuel processes such as methane gas steam reforming and coal gasification in addition to water electrolysis utilizing renewable electricity. While the share of hydrogen production by water electrolysis is currently small, it is projected to grow from about 27 kilotons (kt) to 8 Mt by 2030 with the help of investments from governments all over the world.[6] In addition to the high costs of electrolytic hydrogen, the major roadblock for the hydrogen economy is actually getting the hydrogen to the end user. Creating a hydrogen infrastructure is challenging due to the low energy density of hydrogen and its low boiling point (−253 °C vs −162 °C for methane gas). Hence, hydrogen is mostly produced close to where it is used which is predominantly in petroleum refineries and chemical plants. However, for the widespread use of hydrogen as an energy source, the infrastructure must be improved significantly. In this respect, many methodologies are being explored with a variety of carrier gases such as methane (CH_4) and ammonia (NH_3), which are investigated as possible transportation fuels since pipeline networks already exist allowing for relatively easy transportation in comparison to the transportation of pristine hydrogen.[7–9] The pipeline networks for methane and ammonia extend about 300,000 miles and 2000 miles, respectively.[10–12] The blend of methane and hydrogen is also being explored for hydrogen transportation.[13,14] An advantage of blending hydrogen with ammonia is the increase in combustion energy during power generation. Further, a cost analysis revealed that using liquified carriers are advantageous for long distances

*Electrochemical Society Member.
**Electrochemical Society Fellow.
zE-mail: kramaiyan@unm.edu; rmukundan@lbl.gov

above 1500 km while pipelines are more effective for distances below 1500 km.[15] Clearly, hydrogen, methane, and ammonia could all play pivotal roles in a sustainable hydrogen economy.

Hydrogen is the smallest molecule in existence and while it can be efficiently produced in electrolyzers and converted to electricity in fuel cells, the loss of energy during storage, transportation, and utilization due to leaks is largely ignored today. It is a colorless, odorless, and rapidly diffusing gas making the identification of leaks challenging. Methane has an existing pipeline network for efficient transportation, but this infrastructure also suffers from leaks that are estimated to result in economic losses worth over two billion dollars per year.[16,17] Additionally, methane is a greenhouse gas that is 30 times more potent than CO_2.[18] This means the fugitive emissions of about 3.5% of methane during its extraction from natural gas and processing necessary for the production of hydrogen results in the release of more greenhouse gas than burning natural gas directly.[18–20] Hence, significant effort is also being undertaken to sense methane leaks efficiently or to convert it into higher hydrocarbons to reduce fugitive emissions and flaring.[21,22] The other carrier, ammonia can be harmful to human and animal health if inhaled at concentration levels of 50 parts per million (ppm) over an 8 h period according to the Occupational Safety and Health Administration (OSHA).[23] Key characteristics of all three gases are listed in Table I. One of the key points to note is the large explosion range of hydrogen (lower explosive limit (LEL) 4 vol% to upper explosive limit (UEL) 77 vol%) compared to methane (LEL 4.4 vol% to UEL 17 vol%) and ammonia (LEL 15 vol% to UEL 28 vol%) that should be considered while defining process conditions for mixing hydrogen with either methane or ammonia. For example, it was found that a mixture of 10 vol% H_2 in methane changes the LEL and UEL of methane minimally (LEL 4.2 vol% instead of 4.4 vol%, UEL 18.2 vol% instead of 17 vol%). Hydrogen also has a very low minimum ignition energy (0.017 mJ) compared to methane (0.23 mJ) and ammonia (8 mJ). The comparatively higher LEL (15 vol%) and lower UEL (28 vol%), combined with the higher minimum ignition energy and the higher boiling point makes ammonia very interesting for liquid blends for the transportation of hydrogen. Thus, developing sensors capable of detecting all of these gases in varying concentrations is essential for the successful implementation of the hydrogen economy and to avoid any serious safety incidents. Resolving this transportation problem requires future sensors that are sensitive, selective, fast responding, stable, reliable, efficient, cheap, easily deployable, and mass-producible.

One major development underway is the deployment of Hydrogen Refueling Stations (HRSs) that are being built and made available to consumers at scale in the United States (e.g. California), Japan, Europe, and South Korea to support the introduction of Fuel Cell Vehicles that utilize polymer electrolyte membrane fuel cells (PEMFCs).[24] The hydrogen quality being dispensed is of particular concern because depending on the hydrogen source a large number of impurities have been identified that can impact the performance and lifetime of the PEMFC stack in the vehicle negatively.[25] It is recommended that the hydrogen dispensed to the end-user meets the SAE J2719 standards in the United States (and ISO 14687 Internationally that possess identical specifications as SAE J2719) regarding the maximum allowable concentration of various impurities.[26] Currently, the hydrogen refueling stations are required to periodically analyze the fuel to verify that it meets the purity specifications. Since testing requires time and money, the analysis interval can vary between 2 to 6 months and is required in particular after any changes in the station's configuration when the risk is higher that the fuel is below the desired quality standards. These configuration changes include but are not limited to temporary changes of the hydrogen source, alterations in system's equipment or configuration used for production, compression, or storage. However, even with periodic testing it can take some time to discover quality issues and fuel cell vehicles could get damaged. Therefore, continuous monitoring of hydrogen purity at the station would be a significant improvement and extremely advantageous.[27] Unfortunately, the number of identified chemical impurities that can impact the PEMFC's performance negatively is quite large and, moreover, no single detection technology is capable of sensing all of the various chemical species. These impurities include atomic species (He, Ar), simple diatomic molecules (N_2, O_2), simple covalent molecules (H_2O, H_2S, CH_4, and NH_3), hydrocarbons, halogenated hydrocarbons, more complex molecules like formaldehyde and formic acid (HCHO, HCOOH) as well as solid particulates.

In the wake of these recent developments, there is a renewed need for advances in sensors for the hydrogen economy that are capable of detecting and quantifying hydrogen, methane, and ammonia and the impurities therein. Many sensor types are being developed for the detection of all these gases. The U.S. Department of Energy (DOE) has established targets for hydrogen safety sensors such as the concentration range (0.1 vol% to 10 vol%), the response time (<1 s), and lifetime (∼10 years).[28] However, no such established targets are available for methane or ammonia sensors. The most common sensor platforms include (i) electrochemical sensors, (ii) chemiresistive sensors,[29–31] (iii) combustible gas sensors (CGS),[32] (iv) thermal conductivity sensors (TCS), and (v) optical sensors. Among these sensor types chemiresistive sensors, CGS, and TCS suffer from poor selectivity making them unsuitable for HRS applications where the identification of impurities in a large hydrogen background is essential to monitor fuel quality. Additionally, hydrogen selectivity in air is paramount for safety applications. For example, hydrogen emissions may also have indirect effects on climate change as emitted hydrogen reacts with atmospheric hydroxyl radicals converting them to water vapor, resulting in reduced GHG scavenging as these hydroxyl groups are essential for removing methane and other greenhouse gases, thereby increasing GHG residency time and increasing global warming.[33]

In summary, the direct utilization of hydrogen in PEMFCs and solid oxide fuel cells (SOFCs) as well as the production of hydrogen from polymer electrolyte, liquid alkaline and solid oxide electrolyzers is expected to be at the center of energy conversion processes in the hydrogen economy. As noted above, both methane and ammonia have important roles to play in the production and transportation of hydrogen. Hence, our focus here is to provide an overview of various sensing technologies currently available for these three gases including their working principles, commercialization status, and future prospects. Many review articles are available

Table I. Key characteristics of the three main carrier gases; hydrogen, methane, and ammonia.

Properties	Hydrogen	Methane	Ammonia
Density (kg/m^3)	0.084	0.717	0.86
Boiling point	−253 °C	−161 °C	−33 °C
Odor	No	No	Yes
Lower Explosive Limit (LEL)	4.0 vol%	4.4 vol%	15.0 vol%
Upper Explosive Limit (UEL)	77.0 vol%	17.0 vol%	28.0 vol%
Auto Ignition Temperature (AIT)	560 °C	595 °C	651 °C
Net Heating Value (NHV) (MJ/kg)	143	55	18.8
Minimum Ignition Energy (MIE)	0.017 mJ	0.23 mJ	8 mJ

on hydrogen sensors focused on general applications.[31,34–37] However, there is not a systematic study on sensor requirements for the hydrogen economy with new applications such as fuel cells and electrolyzers combined with carrier molecules such as methane and ammonia. Hence, in this article, we will review the latest developments in sensors for these three gases with a focus on critical applications in the hydrogen economy. We also address the major technological advancements in detecting these gases. Electrochemical (EC) sensors look to be the front runner and provide one of the lowest power approaches while maintaining good analytical performance. However, EC sensors are known to suffer from selectivity problems.[35] The recent research focus on improving selectivity and sensitivity in complex gas environments will be discussed in the concluding part of the article. It is likely that contributions from many sensor technologies including artificial intelligent operation and data interpretation will be needed.

Sensors for the Hydrogen Economy

Hydrogen sensors.—Hydrogen safety sensors have been in commercial use for several decades and numerous comprehensive reviews have been published on the various technologies used to detect hydrogen.[31,34–36,38] Several technologies including electrochemical (amperometric and potentiometric), chemiresistive, optical, thermal, piezoelectric, acoustic, catalytic, and mechanical have been widely studied for this application and Review of Currently Available Commercial Sensors for H_2, CH_4, and NH_3 section has a comprehensive review of several of these technologies that have been used for commercial sensing. A schematic representation of some of these technologies is given in Fig. 1. In this section we provide more details on two of the most widely used technologies for hydrogen sensing, viz: chemiresistive and electrochemical. Recent interest in chemiresistive sensors and electrochemical sensors have surged due to their low detection limits, low cost, and durable sensor designs.

Chemiresistive sensors involving metal oxide semiconductors (MOS) have shown the greatest promise for parts per billion (ppb) level detection.[31,38] MOS-based sensors mainly operate by the reaction of analytes (H_2) with the chemisorbed oxygen species on MOS surface such as O^- and O_2^-. Depending on the MOS type, these oxygen species trap electrons and create electron depletion layers (n-type MOS) or hole accumulation layers (p-type MOS) resulting in the formation of Schottky barriers. Upon reaction with hydrogen, these oxygen species form H_2O and release electrons back into the MOS, thereby changing the Schottky barrier height which can be observed as a resistance change.[39,40] MOS-based sensors typically operate at higher temperatures that require high power consumption. Novel MOS materials have been developed recently to detect ppb levels of hydrogen in a laboratory setting.[41,42] Similarly, recent innovations in two-dimensional (2D) materials have shown great potential for gas sensing applications due to their large specific surface areas and strong surface activities.[43–46] For example, a 2D vanadium carbide MXene was recently shown to have a low limit of detection of 2 ppmv for hydrogen.[47] However, the primary drawback of this technology is the cross interference from other common atmospheric gases and humidity. A detection limit of 10 ppbv was demonstrated utilizing ceria loaded indium oxide hollow spheres.[41] The detection of 50 ppbv H_2 was demonstrated with a MOS based sensor utilizing Pd nanoparticles mixed in with an indium oxide material containing zinc oxide nano-fibers.[42] A theoretical detection limit of 10 ppbv was achieved by the incorporation of Pd nanoparticles on zinc oxide nanoflowers based MOS in chemiresistive sensors.[48] Incorporation of Pd nanostructures is commonly seen to enhance the sensitivity and selectivity of many hydrogen sensors as Pd enables a nearly barrierless hydrogen dissociation to chemisorbed hydrogen atoms on its surface.[49,50] Response and recovery times of 1 s and 10 s have been demonstrated for the ceria loaded

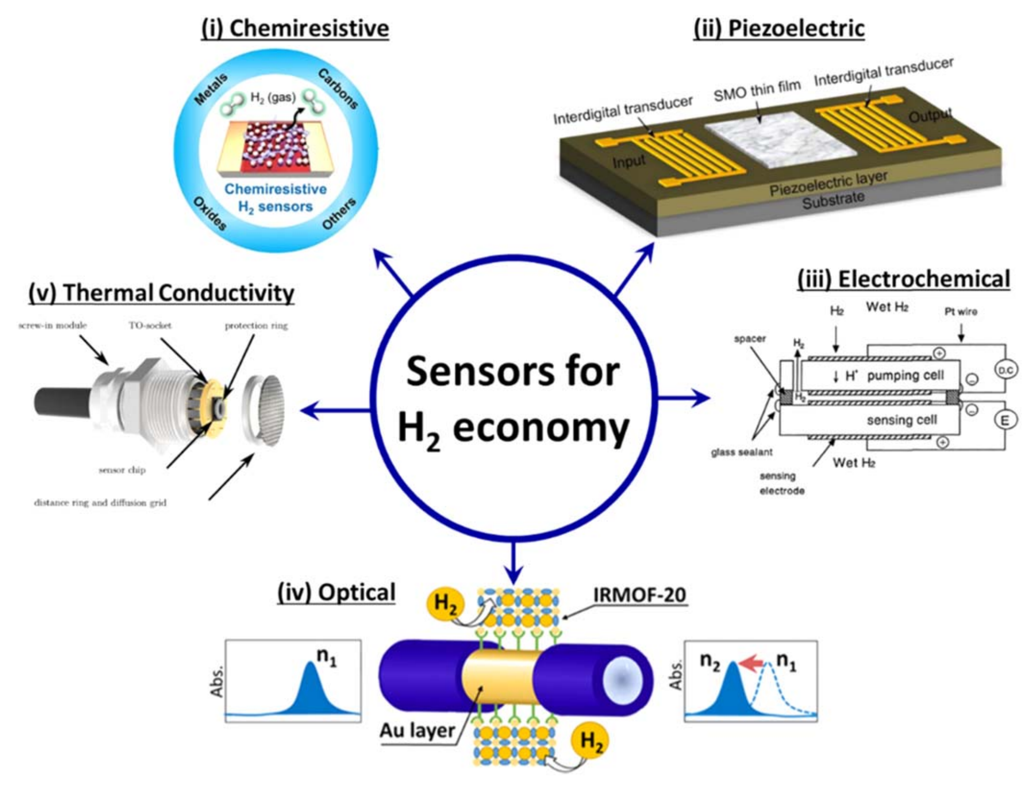

Figure 1. Schematic illustration of some of the hydrogen sensing technologies available in the literature with sample examples (i) Chemiresistive H_2 sensors (adapted with permission from ACS Nano 2020, 14, 11, 14284–14322. Copyright 2020 American Chemical Society.[39] (ii) Piezoelectric sensors (reprinted from Ref. 38 with permission from Sensors 2012, 12, 5517, MDPI), (iii) Electrochemical sensors (Reprinted from Ref. 51, Copyright 2001 with permission from Elsevier) (iv) Optical sensors (Reprinted with permission from ACS Sensors, 2019, 4, 3133, Copyright 2019 American Chemical Society)[52] (v) Thermal conductivity sensors (Reprinted from Ref. 53, Copyright 2020 with permission from Elsevier).

indium oxide hollow sphere sensor at an operating temperature of 150 °C.[41]

Electrochemical sensors, due to their potential to operate in a wide temperature and concentration range, offer flexibility towards specific applications. Electrochemical sensors can be broadly classified into three categories, (i) potentiometric, (ii) amperometric, and (iii) conductometric. Conductometric gas sensors are rare on the commercial sensor market and therefore will not be further discussed in this review. Potentiometric and amperometric electrochemical gas sensors are significantly more relevant on the sensor market and the fundamental equations used for their evaluation are summarized in Table II. An electrochemical sensor has at least two electrodes: an anode where the oxidation takes place and a cathode where the reduction takes place. In the case of hydrogen detection, H_2 is oxidized to H^+ at the anode, while O_2 is reduced to H_2O at the cathode. Since the sensing reaction with the target gas takes place at the anode, this electrode would be considered the working electrode (WE), while the cathode would be considered the counter electrode (CE). However, in a two-electrode setup the counter electrode is also the reference electrode (RE). This can work acceptably well for potentiometric sensors where a change in potential is measured. For amperometric gas sensors, however, a non-polarizable reference electrode is needed where a constant potential can be applied while a change in current between the working and the counter electrode is measured. Potentiometric sensors offer the choice for miniaturized sensors as the potential generated is controlled by the Nernstian equation that is independent of the electrode size. In amperometric gas sensors, the measured sensor signal is current, and is generated by the reaction of hydrogen at the sensing electrode. Operation of these sensors under diffusion-limited conditions provides a direct proportional relationship between current and the analyte hydrogen concentration. A new type of sensing, the mixed potential sensing phenomenon is often observed in high-temperature solid electrolyte sensors where the sensing electrode (SE) is exposed to reducing gases such as CO and H_2.[54–56] As a result, more than one redox reaction occurs at the SE leading to the generation of mixed potential. When the exchange current densities for the redox reactions are equal, the mixed potential is attained and the device response potential is the difference in the mixed potential obtained at each electrode. As a result, mixed potential electrochemical sensors (MPES) can work in single chamber configurations where both reference electrode and sensing electrode are exposed to the same gas environment.[55] The difference in kinetics towards each redox reaction for the individual electrode determines the sensor response. Hence, the choice of electrode and its geometry are important characteristics for achieving reliable sensor response.[57,58]

Electrochemical hydrogen sensors depending on the choice of electrolyte and mode of operation, can offer a wide range of operating temperatures and provide one of the lowest power consumption approaches using low-power simple circuits. Low-temperature operation involves liquid and polymer-based electrolytes while high temperature operation involves ceramic metal oxide electrolytes. The most commonly used liquid electrolyte for hydrogen sensor application is H_2SO_4 which is normally distributed in porous membrane matrixes such as Teflon or silica to reduce electrolyte evaporation. Major requirements for a successful hydrogen sensor of this type are (i) selectivity towards hydrogen in environments with cross interferents, (ii) stable and reproducible sensor response. Traditional sensor configurations utilized Pt as the reference electrode due to its fast kinetics towards hydrogen electrooxidation. However, Pt electrodes suffer from significant drift in measured potential due to hydrogen adsorption on the electrode. Chao et al. have demonstrated that by changing the design and choice of reference electrode, both these challenges could be solved.[35,59] In a conventional three electrode sensor with H_2SO_4 electrolyte, installing a fluoroethylene propylene membrane in the gas inlet prevented common interferent gases such as CO while H_2 permeated easily improving selectivity. The problem of hydrogen induced potential drift associated with Pt reference electrode was addressed by utilizing a Nafion® coated Ag/AgCl wire as the reference electrode. The incorporation of Nafion® coating helped prevent the transport of chloride ions and cations between the electrolyte and RE providing a stable potential. hydrogen sensor fabricated with this configuration showed a reversible drift-free response and negligible cross-sensitivity to CO, NH_3, and H_2S.[59] Nafion® coated Ag/AgCl reference electrode was also utilized to explore the hydrogen sensing property of a PdO deposited reduced graphene oxide (rGO) composite electrode recently, although the recovery time for the PdO/rGO sensor was comparatively higher.[60]

Compared to liquid electrolytes, solid polymer electrolytes have advantages such as leakage free operation, reduced corrosion, and volatilization, but suffer from changes in conductivity with relative humidity (RH) change and membrane-water freezing at low temperatures with subsequent loss of conductivity. For hydrogen sensors based on solid polymer electrolytes, perfluoro sulfonic acid membrane is the widely used electrolyte although polybenzimidazole (PBI) and sulfonated polyether ether ketone (S-PEEK) have also been explored.[35] Many recent efforts focus on Nafion® as the electrolyte with Pt and Pd as sensing electrodes.[61–64] A Pd on carbon fiber (Pd/CF) with varying Pd loading (5, 10, and 20 wt%) was utilized recently with Nafion® membranes where the 10% Pd/CF showed a linear sensor response to H_2 concentration in the range of 200–10000 ppmv with a sensitivity of 0.0131 μA/ppmv H_2.[61] Due to their resemblance to PEMFCs, this particular design has been tested for hydrogen sensing in conditions relevant for PEMFC operation. The next section describes some recent developments using this particular type of sensors for accessing hydrogen quality. An overview of commercially available electrochemical hydrogen sensors is presented in Review of Currently Available Commercial Sensors for H_2, CH_4, and NH_3 section.

Sensors for hydrogen refueling stations.—The aforementioned hydrogen sensors focus on measuring the hydrogen concentration in a given environment, either resulting from a leak or in a gas stream. However, at HRSs, there are two types of sensors required, one for the detection of hydrogen leaks and one for the quality control of hydrogen. The various effects of impurities in hydrogen on the performance of PEMFCs have been studied in depth over the years.[65–74] The mechanism of poisoning typically involves the adsorption of impurities onto the anode's platinum (Pt)

Table II. Operating principle of potentiometric and amperometric sensors.

Potentiometric sensors	Amperometric sensors
$E = E^o + \frac{RT}{nF} \ln \frac{P_x}{P_{ref}}$	$I = nFQC$
R–gas constant,	I—current (coulombs/s),
F—Faraday constant,	Q—rate of gas consumption m^3/s),
T—temperature (K).	F—Faraday constant,
n—number of e involved in the redox reaction,	n—number of electrons involved in the redox reaction.
P_x—Partial pressure in sample gas mixture.	C—concentration of the analyte gas (mol/m^3)
P_{ref}—reference partial pressure.	

electrocatalyst, thus blocking sites for the hydrogen oxidation reaction (HOR) and lowering the PEMFC's performance.[66] Moreover, impurities are also known to infiltrate the membrane as ions, decreasing its conductivity. Some impurities have also been observed to cross over to the cathode side of the fuel cell and to adsorb on the Pt cathode, inhibiting the oxygen reduction reaction (ORR). The effects of impurities on the fuel cell's performance depend on the operating mode of the fuel cell as well as the type of impurity.[74] For example, it has been shown that ammonia lowers the membrane's conductivity and cannot be easily reversed without flushing the ammonium cations out of that ion-exchanged membrane.[70] The effects of some impurities are reversible, meaning that the cell's performance can be fully recovered when the impurity is removed and clean hydrogen is introduced.[71,72] Impurities like CO,[67] and H_2S,[69] for example, adsorb onto the Pt electrocatalyst and can be easily desorbed when the operating potential of the anode is increased during the start-up and shut-down period. Hence, a simple, reliable, and inexpensive set-and-forget sensor system for detecting contaminants in hydrogen would reduce operating costs for the HRS station operators and remove the necessity for complex instrumentation.[27]

Recently, many types of sensors for humidity, oxygen and dew point are being developed and marketed for the detection of impurities in hydrogen. These sensors were listed in a recent review, though their application success is not yet known.[75] In this section, we focus on a recently developed electrochemical hydrogen fuel quality sensor or hydrogen contaminant detector (HCD) developed by Los Alamos National Laboratory (LANL) as a possible solution for HRSs. The HCD is designed to continuously monitor fuel quality at the HRS based on CO levels as sentinel species and to alert the station operator in case the CO level rises above the permitted level in a hydrogen fuel stream.[76] The device's ability to detect H_2S has also been demonstrated. The HCD is based on a hydrogen pumping cell with an ultra-low Pt loaded working electrode, which means the HOR is very sensitive to contaminants. This includes not only CO and H_2S, but also any other impurity that inhibits the HOR like for example ammonia poisoning.[77] The key novelty of this device compared to other electrochemical ones is the use of a patented Nafion® 117 membrane system including a water wicking system for humidification that enables the operation of the hydrogen pumping cell in a dry hydrogen environment. The patented membrane system in combination with a pulsed operating mode results in exceptional long-term stability and durability.[77] A similar methodology was utilized by Noda et al., where the potential instead of the current was monitored as impurities were introduced.[78,79] The utility of this HCD shown in Fig. 2a was successfully demonstrated in a field test at the H2Frontier hydrogen refueling station in Burbank, CA USA. The HCD was operated at an applied potential of 0.1 V with periodical short exposure to 1.5 V that ensured the removal of any accumulated impurities. The current measured at 0.1 V for a fixed time is used to make an impurity determination whereas the short exposure to 1.5 V effectively re-sets the HCD. HCD current response obtained for such a pulsed polarization protocol (PPP) is shown in Fig. 2b where a dramatic difference in HCD response is observed following the introduction of H_2 contaminated with 200 ppb of CO. Figure 2c illustrates the response of this HCD after an actual restart of the steam-methane reformer system (SMR) at the HRS clearly demonstrating the high levels of CO produced after a SMR restart and the continuous reduction in CO levels due to the pressure swing adsorption (PSA) system that removes all remaining traces of CO before storage of the hydrogen. A planned introduction of 1 ppmv CO in H_2 indicated that the CO levels during the restart of the SMR are much higher than permitted by SAE J2719 and that the HCD is capable of detecting these levels with the above described operation protocol.[77] The HCD when exposed to roughly 10 ppb H_2S (2.5x SAE J2719 standard) produced a comparable electrochemical impedance spectroscopy (EIS) response behavior as observed with CO, indicative of contaminant binding to the Pt catalyst in the WE although with a significantly slower electrode kinetics (Fig. 2d).[77] It should be noted that since this detector is constructed with components that are similar to those actually used in a PEMFC (membrane, electrocatalyst, catalyst support, and ionomer) stack, it would be capable of detecting any impurity that poisons any of these components irrespective of the poisoning mechanism. The identification of ammonia contamination is theoretically possible because ammonia will lead to an increase in the high frequency resistance (HFR) which will not be observed for either CO or H_2S.[77] For example, introduction of 25 ppmv NH_3 in a H_2 feed has shown to increase the HFR from 0.10 $\Omega \cdot cm^2$ before ammonia exposure to 0.25 $\Omega \cdot cm^2$ after 15 h of ammonia exposure.[80] A recent study demonstrated a similar increase in HFR after exposure to 10 ppmv NH_3 although the duration of exposure is not clear.[81]

The potentiometric sensors developed by Noda et al.[78] have similarly detected the introduction of 0.5 ppmv CO and 0.5 ppmv H_2S into the hydrogen fuel feed. The potential drop is well pronounced in sensors with lower Pt loading (0.015 $mg\ cm^{-2}$) in comparison to sensors with higher Pt loading (0.05 $mg\ cm^{-2}$).[78] Introduction of 5 ppmv ammonia was found to affect both high and low Pt loaded sensors equally, suggesting that ammonia poisoning is associated with lowering the membrane conductivity rather than blocking the Pt sites. Other types of sensors such as optical sensors and mobile-gas chromatography are being developed as well for this application. An optical sensor based on laser-induced breakdown spectroscopy was demonstrated to detect N_2, O_2, Ar and He in H_2 fuel at concentrations below 100 ppmv.[82] A hydrogen impurity analyzer based on mobile gas chromatography was found to detect O_2, Ar, N_2 and CH_4 in an H_2 stream at concentrations below 3 $\mu mol\ mol^{-1}$.[83] There clearly is a need for reliable quality control to ensure that hydrogen fuel cell based vehicles do not get their fuel cell stacks poisoned with contaminants and lose performance. The current available technologies allow for periodic testing, however, continuous monitoring of a broad range of contaminants is required. Further research is needed to obtain the sensors that can readily detect a wider variety of contaminants in the hydrogen fuel and fulfill this need.

Sensors for methane and methane/hydrogen blends.—The transportation of hydrogen requires either the buildup of new transportation infrastructure, conversion of hydrogen into easier to transport fuels, or the use of existing fossil energy transportation networks. The US has over 300,000 miles of existing natural gas pipelines.[10] Instead of transporting pure hydrogen, it can be blended with methane at concentrations up to 25 vol% H_2 while still being able to be transported in the established natural gas transmission system.[14,84] This mixture attracted commercial attention by many companies and is trademarked in the name of Hythane™.[85,86] A technoeconomic analysis by Di Lullo identified hydrogen-methane blends and pure hydrogen pipelines as the lowest cost methods for long-range transport of hydrogen if the output pressure of H_2 is kept $<$35 psi.[87] The extensive network of natural gas pipelines available for repurposing towards hydrogen-methane blends transportation comes with the associated safety risks and greenhouse gas emissions due to using old infrastructure. The current survey methods carried out by natural gas companies involve walking surveys with handheld meters that detect leaks.[88] There is currently no widely deployable sensor technology for continuous monitoring of hydrogen, methane or hydrogen-methane blends leakage. In this section, we will review methane sensors and discuss their integration into combined H_2/CH_4 sensing systems. Figure 3 shows some examples of sensors used in the detection of methane.

Methane monitoring is often performed using optical monitoring methods. Methane absorbs in the infrared spectrum at 2.3 and 3.3 μm and infrared (IR) absorption methods have been developed for its detection at these wavelengths. Diatomic molecules like H_2 do not absorb IR and selectivity for methane vs hydrogen is excellent. Methods for methane detection have been developed using non-dispersive infra-red (NDIR),[91–93] cavity ring-down spectroscopy (CRDS),[94–96] tunable laser diode,[88,97–99] and photoacoustic

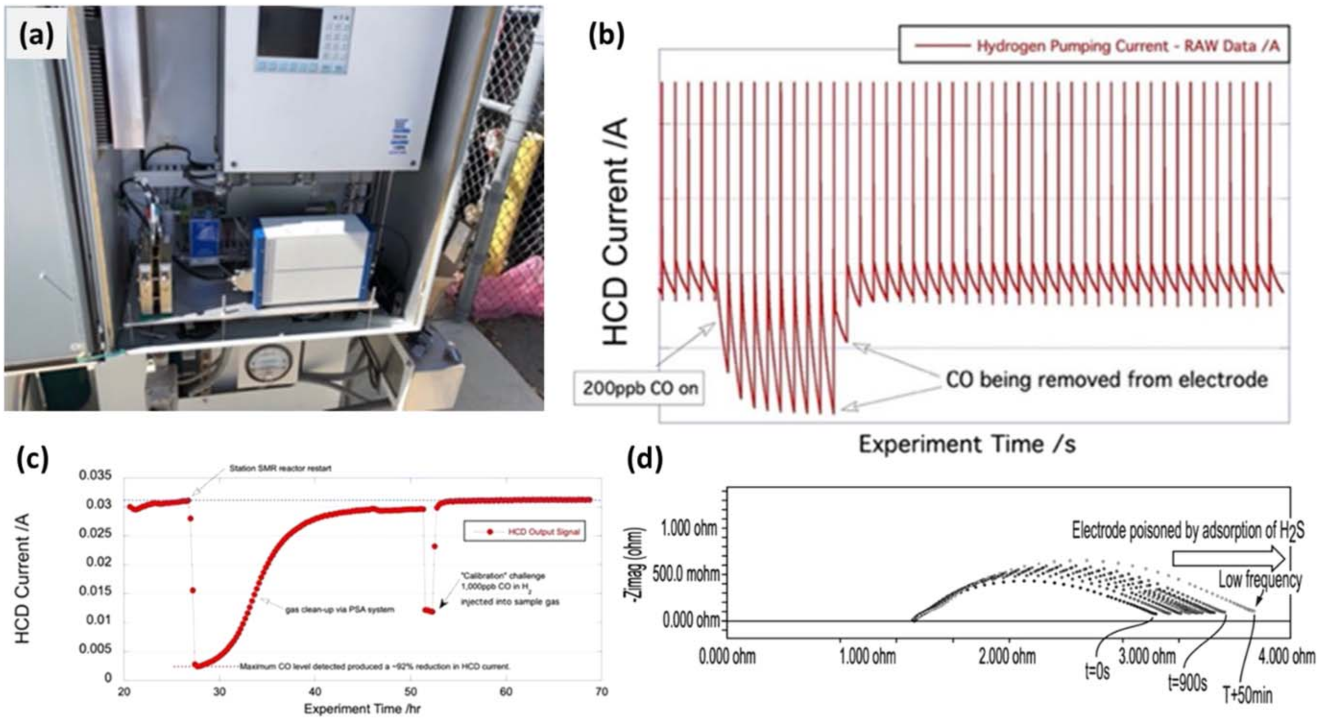

Figure 2. (a) Field testing an experimental HCD system (HCD, flow controller, and potentiostat) at the H2Frontier hydrogen refueling station located in Burbank, CA. (b) Generalized hydrogen pumping current behavior during HCD operation. The working electrode is stripped of CO at 1.5 V and current peaks after a longer period of time at 0.1 V. The current at 0.1 V always shows decay due to the accumulation of ultra-trace level impurities that interfere with hydrogen oxidation reaction however a significantly larger decrease in current is measured when 200 ppbv CO (the SAE J2719 standard) is introduced to the hydrogen sample gas stream. (c) Data collected at H2Frontier filling station in Burbank, CA during steam methane reformer (SMR) restart. The HCD qualitatively tracked level of CO contamination as H_2 station production reached optimized operating efficiency. (d) Electrochemical Impedance Spectroscopy (EIS) data from 150 kHz to 1 Hz collected as a function of exposure time for 10 ppbv H_2S.

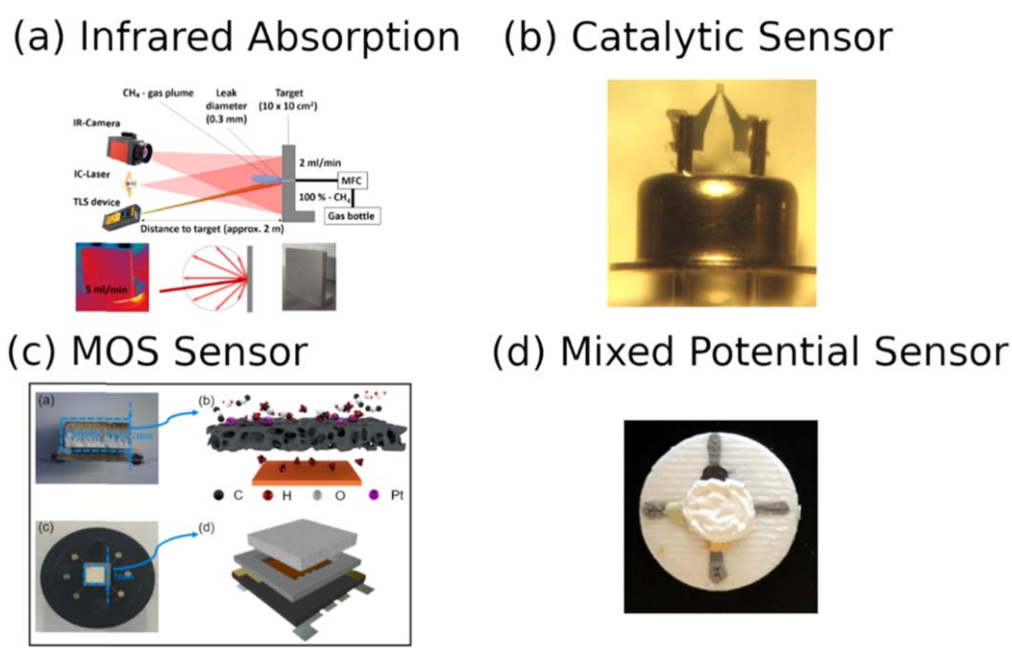

Figure 3. Four different types of methane detection technologies. (a) Tunable laser infrared absorption sensing of a methane leak. Reprinted from Ref. 88 and with permission via the OSA Open Access License. (b) A miniaturized low-power Pd-Pt catalytic sensor. Reprinted from Ref. 89 with permission from Elsevier. (c) A SnO_2 metal-oxide semiconductor (MOS) sensor with a catalytic PtO-Al_2O_3 filter to improve selectivity towards methane. Reprinted from Ref. 90 with permission from Elsevier. (d) A mixed potential sensor containing Pt, Indium tin oxide (ITO), $La_{0.87}Sr_{0.13}CrO_3$ (LSC), and Au electrodes for methane gas detection. Reprinted from Ref. 16 with permission via CC-BY license.

sensing.[100–103] Detection of methane alone is insufficient to confirm the presence of a natural gas leak since methane occurs naturally. IR methods have also been developed that simultaneously quantify methane, ethane, and propane which are present in natural gas but not in other methane sources such as wetlands or agriculture.[101,104–107] For example, Control Measure Regulation

(CMR) group has launched a near infrared intelligent sensor (NIRIS) for natural gas that can speciate methane, ethane, and propane and measures the composition of natural gas in real-time.[107] However, the measurement range for methane is 50–100 vol% that is suited to optimize the fuel consumption than natural gas leaks. Also, gas pipelines with varying hydrogen concentrations can act as a diluent to the IR-active methane and can lead to measurement errors. Another option is isotopic analysis by both CRDS and photoacoustic methods sensitive enough to distinguish the expected C isotope distributions from different sources.[108,109] IR measurement techniques have also been widely deployed on manned and unmanned aerial surveys of emissions from existing natural gas infrastructure.[110–112] While IR methods have been extremely sensitive and selective for natural gas emission studies, the requirements to keep optical cavities clean and free from dust, and keeping IR transparent windows stable in changing RH, make their long-term deployment challenging for continuous monitoring applications.

Catalytic sensors for methane detection are widely deployed in a safety context where they detect the concentration of flammable gases in air (O_2 is necessary for operation) when it rises above their LEL.[113,114] The increase in temperature during the exothermic oxidation reaction of methane on a hot catalyst (Pt or Pd) coated temperature transducer is used as a sensing parameter. Typical detection ranges are in the 100's of ppmv to 4 vol% LEL for methane.[89,115,116] Park et al. demonstrated a dual Pd/Al_2O_3 and Pt/Al_2O_3 catalytic sensor that could detect total concentrations for CH_4, H_2, and binary mixtures of $CH_4 + H_2$ in the 200–2000 ppmv range.[116] Miniaturization of catalytic methane sensors with feature sizes on the order of 100's of microns have been shown to reduce the power needed for heating the oxidation catalyst. Karpov et al. demonstrated a device that could sense methane at 0.2–2.5 vol% range while operating on 1.2 mW of power.[89]

Solid-state electrochemical sensors have been widely investigated for methane and hydrogen detection and are expected to have lower power and cost than IR methods. Hydrogen is commonly studied as cross-interfering species in electrochemical and MOS methane sensors but not NDIR. Sensors for methane include metal-oxide semiconductor sensors and mixed potential electrochemical sensors. In a metal-oxide semiconductor sensor, the reaction of interest is the reaction of methane with oxygen within or adsorbed at the MOS surface (Eq. 1):[117,118]

$$CH_4 + 4O^- \rightarrow CO_2 + 2H_2O + 4e^- \quad [1]$$

This reaction results in a decrease in the resistance of the metal-oxide layer (for n-type semiconductors) and resistance change is used as the sensor response. Recent efforts in producing doped metal oxide-based nanostructures have yielded improvements in methane sensitivity. The typical range of detection for metal oxide semiconductor sensors using SnO_2 as sensing material is in the order of 10–10,000 ppmv CH_4.[119] Nanostructured ZnO semiconductor sensors were studied and had a reported detection range of 0.01–1 vol% CH_4.[117,120] Pd-doped SnO_2 was used to detect methane in the range of 25–1,000 ppmv with 6–7 times enhanced response compared to pristine SnO_2.[121,122] Pt-modified SnO_2 sensors showed a range of sensitivity between 25–930 ppmv.[123] In environments containing both methane and hydrogen, the selectivity of the semiconductor sensor can be controlled by surface modification and catalytic coatings. The majority of the work has been focused on increasing the selectivity to hydrogen against methane and other hydrocarbons. Hexamethyldisiloxane modification of a SnO_2 sensor resulted in a sensor not responding to CH_4, CO, and heavier hydrocarbons but to H_2 with a limit of detection of approximately 250 ppb.[124] Similar success was achieved using Au nanoparticles on SnO_2 to promote sensitivity to hydrogen over methane with a limit of detection of 400 ppb.[119] Catalytic filters have been demonstrated to enhance the selectivity of semiconductor sensors for methane over other hydrocarbons and NO_x species by reacting away unwanted species.[90,125,126] A field demonstration of MOS based sensors for the detection of methane was successfully able to measure methane emissions from a simulated underground natural gas pipeline leak at rates of 0.042 and 0.127 kg h^{-1}.[127]

Mixed potential electrochemical sensors have been investigated for methane sensing. The electrochemical half reactions are expected to be the oxidation of methane (Eq. 2) and the reduction of oxygen (Eq. 3):

$$CH_4 + 2O^{2-} \rightarrow CO_2 + 2H_2O + 4e^- \quad [2]$$

$$O_2 + 4e^- \rightarrow 2O^{2-} \quad [3]$$

Sekhar et al. showed indium tin oxide (ITO) vs Pt in a yttria-stabilized zirconia (YSZ) solid electrolyte to have high selectivity towards 100 ppmv CH_4 vs CO, H_2, CO_2, and NO_x, but weaker selectivity against C_3H_6.[128] They reported a four times higher sensitivity to methane when applying a pulse discharge method. Halley et al. developed an additive manufacturing process for the production of a four-electrode Pt, $La_{0.87}Sr_{0.13}CrO_3$, ITO, and Au mixed potential electrochemical sensor and demonstrated the ability to identify 1,000–4,000 ppmv of simulated natural gas mixtures, CH_4 only, and agricultural simulants containing CH_4 and NH_3.[16] Yang et al. showed high selectivity for methane using a $SmMn_2O_5$ electrode against Pt with YSZ as solid electrolyte in a mixed potential electrochemical sensor achieving a lower detection limit of 25 ppmv CH_4.[129]

The current drivers for future developments in methane sensing are reduced cost, lower power, increased durability (long lifetime), stability (no need for compensations or periodic calibrations), specificity towards the target species (methane or hydrogen), and improved sensitivity for environmental monitoring to perform both identification and quantification of leaks. For example, satellite-based survey methods recently demonstrated the significant underestimation of methane leaks from industrial sectors but it is not a suitable method for leak site identification.[130] Hence, more specifically, the current requirements for electrochemical sensors with improved stability require limits of detection at the 1 ppmv level.[131] Tian et al. have estimated that a minimum of 6 h of continuous monitoring are needed to accurately predict a leak rate from an underground methane source by atmospheric sampling.[132] Few efforts have investigated sensors that can simultaneously quantify mixtures of methane and hydrogen. In the research reviewed above, the two gases are typically treated as interferent species and selectivity is tuned to either methane or hydrogen, but not both although some limited examples are given in Multi-Sensor Arrays, Electronic Noses, and Machine Learning for Hydrogen Sensing section. The successful monitoring of emissions leaking from hydrogen-methane blends or natural gas-derived hydrogen infrastructure will require sensors that can simultaneously quantify both species. Multi-sensor arrays (electronic noses) integrated with machine learning methods are a promising solution to this, where response from different sensors with varying selectivity towards hydrogen and methane could be used to deconvolute the composition (see Multi-Sensor Arrays, Electronic Noses, and Machine Learning for Hydrogen Sensing section). Again, AI interpretation of complex sensor data is a promising direction to achieve improved specifications for future sensors.

Hydrogen as an Interfering Gas

The use of gas sensors for monitoring the environment as part of a broader Internet of Things (IoT) approach to improving the quality of life is constantly increasing.[133] The market size of gas sensors that monitor indoor air quality (IAQ) for homes and hospitals, outdoor environments for cities and farms, and toxic gases and other pollutants for industry is expected to grow in the coming decades.[133] However, the impact of the hydrogen economy on these sensors is not understood and needs to be addressed to ensure a smooth transition to smart clean technologies. The primary impact of the hydrogen economy on smart sensors will be its presence as an interfering gas to the intended response of IAQ sensors. Current standards for most sensors in use today do not consider hydrogen as an interfering gas, since its presence is not prevalent in the environments where these sensors function.[134] However, the recent use of rechargeable lead acid battery systems has created a situation where hydrogen can be released into an indoor environment during the charging process.[135] This accidental release of hydrogen has already resulted in false alarms of existing CO sensors and has been the subject of a 2019 publication.[136] In this section we will review the publications related to the impact of hydrogen on some sensors that are currently being considered for monitoring indoor air quality.

Several low-cost sensors including NO_2, O_3, CO_2, CO, t-VOC (total-volatile organic compounds), PM (particulate matter), radon, SO_2, and H_2S sensors have the potential to be used for indoor air quality monitoring.[137] The operating principles of these sensors vary widely and could be based on one of several sensing mechanisms including electrochemical, chemiresistive, photoionization (PID), infrared, optical, catalytic bead, thermal conductivity, or piezoelectric/pyroelectric. The impact of hydrogen gas on the response depends on the sensing principle and is expected to play a significant role in primarily chemiresistive, electrochemical, catalytic bead and thermal sensors. For example, when seven commercially available CO sensors were evaluated with 100, 200, and 500 ppmv H_2, all but one of them resulted in false CO alarms.[136] Considering that the LEL of H_2 is 4 vol%, and most safety systems will not alarm below 20 vol% LEL or 8000 ppmv, it is definitely possible for indoor hydrogen concentrations to routinely exceed 500 or even 1000 ppmv without any safety implications. Therefore, it will be critical to ensure that other sensors in that environment can operate reliably in a background of approximately 500 to 5000 ppmv of H_2.

Chemiresistive sensors can respond to CO, VOCs, and all combustible gases including hydrogen and will need to be carefully designed to mitigate hydrogen interference. MOS sensing elements are widely used in VOC sensors[138] and CO sensors[139] and are as such commercially relevant even though they are susceptible to hydrogen interference. As described in the previous section, the presence of hydrogen can decrease the amount of adsorbed oxygen on the surface of a MOS-based sensor resulting in a decrease in resistance. This decreased resistance would result in a false sensor reading whose magnitude will depend on the exact sensor utilized. The effect of the interference can be lowered by either using a filter or by using multiple sensors with modified surface coatings that can increase or decrease the sensitivity to hydrogen. Filters are routinely used in MOS sensors to provide better selectivity[140,141] and in specific, a $BaTi_{0.95}Rh_{0.05}O_3$ layer can be used to provide selectivity towards CO in the presence of H_2.[142] Moreover, activated charcoal filters are routinely used in MOS based CO sensors to provide selectivity against absorbable VOCs. As an alternative to filters, additives like noble metals could be used to modify the intrinsic selectivity of the used MOS materials.[143] Specifically, as earlier noted, addition of Pd has been shown to improve the hydrogen sensitivity of a MOS based chemiresistive sensor.[42] While these individual methods result in improved selectivity, they are not ideal solutions since the concentration of hydrogen could significantly exceed the concentration of the target gas. Therefore, multiple sensors or sensor arrays with different selectivities to CO/VOC and hydrogen can be utilized to further compensate the interfering effect of hydrogen.

Electrochemical sensors are also subject to interference from hydrogen which can be electrochemically oxidized at the working electrode of the sensor resulting in a sensor signal that can be mistaken for the target gas. The influence of hydrogen on the response of electrochemical CO sensors has been evaluated in detail in a recent publication.[144] The authors reported significant interference with just 500 ppmv of H_2 (false CO readings from 100 to 150 ppmv) and "out of range" readings for 2 vol% H_2 (50%LEL). The CO sensor's response to hydrogen was also found to change with time impacting the lifetime of the sensor with its hydrogen response decreasing at a faster rate than the CO response with ageing. The incorporation of additional electrodes can be utilized to further decrease the H_2 interference by correcting the signal for CO from one electrode pair with the total H_2+CO response from the other electrode pair. These multi-electrode electrochemical sensors are commercially sold as CO/H_2 low or CO/H_2 Null sensors. Changing the electrocatalyst from Pt to Pd or Au for an H_2 sensor can also virtually eliminate the CO signal.

Catalytic bead sensors are also widely used in combustion gas sensing due to their sensitivity to LEL levels, long lifetime, and relatively low cost.[145] These sensors will invariably respond to hydrogen since it can be oxidized on the catalyst bead that surrounds the Pt wire that acts as a Pt-resistance thermometer. Catalytic bead sensors are widely used as hydrogen LEL detectors in indoor and outdoor environments but do get saturated at high concentrations of H_2 and low oxygen levels. Therefore, these sensors will not be suitable for t-VOC detection in indoor environments where a significant hydrogen concentration is expected. On the other hand, IR-based detection technologies that are currently being used for indoor air quality monitoring (CO_2, VOCs) are not susceptible to interference from hydrogen.[146] Other technologies including Photoionization detectors (PID) and tunable diode lasers that are used for t-VOC and individual gas detection respectively are also immune to interference from hydrogen and offer promising alternatives for indoor air quality monitoring in the presence of significant hydrogen concentrations.[146,147]

Multi-Sensor Arrays, Electronic Noses, and Machine Learning for Hydrogen Sensing

Sensor arrays are used where multiple gas species must be quantified simultaneously or cross interference between sensed species is present. The term "Electronic Nose" originates from the senses in biological noses where multiple signals generated by an array of receptors interacting with aromatic molecules are combined to produce the sensation of smell in the brain.[148–151] Following this analogy, multiple sensors can be combined to produce multidimensional signals from complex chemical mixtures. Sometimes these signals can be deconvoluted mathematically in n-dimensional space and produce identification and quantification for some or all of the gas species present in the sample. Electronic noses have been developed for hydrogen sensing since hydrogen's high reactivity makes discriminating it from other combustible gases challenging with currently available single sensor approaches. A chemically sensitive field effect transistor (FET) array was developed for H_2, CO, CH_4, and liquefied petroleum gas.[152] FET based sensor arrays were also used to quantify simultaneously mixtures of NH_3 and H_2 at the 3–10000 ppmv and 10–10000 ppmv levels respectively.[153] Sensor arrays that can quantify humidity have also been developed and limits of detection of 12 ppmv for H_2 and 30 ppmv for CO were demonstrated once humidity effects were compensated.[152] Sysoev et al. developed a nanowire-based SnO_2/TiO_2/Ni-SnO_2 semiconductor sensor capable of discriminating between H_2 and CO at the 10^{-2} Pa partial pressure range.[154]

An example for sensor array related to hydrogen and hydrocarbons is shown in Fig. 4[155] that was developed as a "Lick and Stick" leak detection system which can be stand-alone and be applied wherever necessary.[156] The complete electronics system with hydrogen, hydrocarbon (see Hydrogen Sensors in Air Transportation Applications section) and oxygen sensors is shown in Fig. 4a. Testing results of a prototype model of the "Lick and Stick" sensor system is shown in Fig. 4b which highlights the response of the SiC-based gas sensor at various hydrocarbon jet fuel (RP-1) concentrations and under constant oxygen concentration. The hydrocarbon sensor, a silicon carbide (SiC) Schottky diode, detects fuel concentrations from 300 ppmv to 3000 ppmv. The hydrogen sensor signal shows no response, suggesting a lack of cross-sensitivity between the hydrogen and hydrocarbon sensors to the detection of this fuel. This example demonstrates the ability to

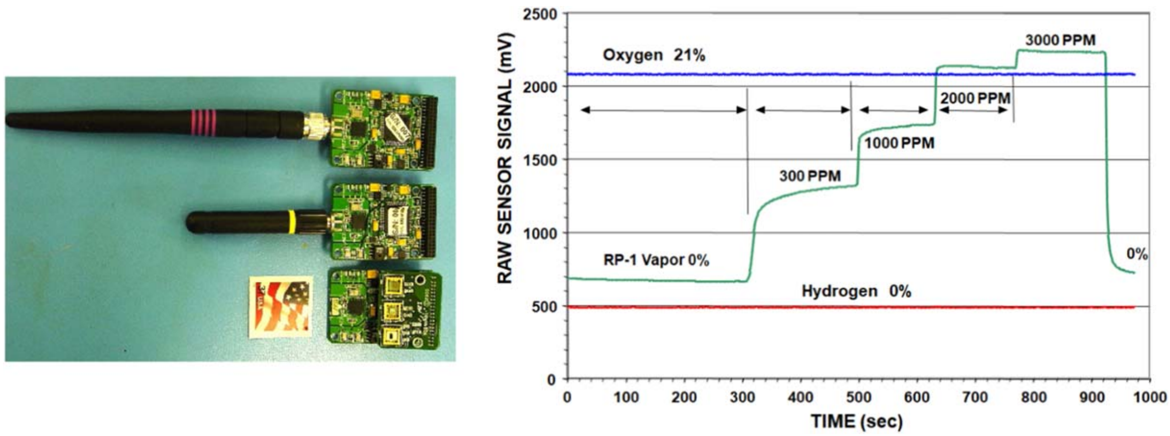

Figure 4. (a) "Lick and Stick" leak detection system configured with different wireless antennae and a hydrogen, hydrocarbon, and oxygen sensor. (b) Response of the three sensors, (hydrogen, hydrocarbons, and oxygen) to a constant oxygen environment and varying hydrocarbon (RP-1) concentrations. The sensor signal shown is the output from the signal conditioning electronics which processes the measured sensor current at a constant voltage (Ref. 155).

integrate these three sensors into a complete sensor array with a full complement of supporting sensor electronics and hardware. Another example of this sensor array approach is where an array of SiC Schottky diode sensors were used for methane, formaldehyde, and acrolein for first responder safety applications.[156]

Figure 5 presents some examples of machine learning and sensor modeling in the gas sensing space. Machine learning (ML) methods are commonly used to analyze sensor signals to perform identification and quantification of gas species in mixtures.[158] The use of artificial neural networks (ANNs) paired with sensor arrays was studied as early as 1991 where an array of Metal Oxide Semiconductor Field Effect Transistors (MOSFET) sensors was used to quantify concentrations of H_2/NH_3 and H_2/Acetone mixes.[159] In the three decades since this early work, advances in computing power, the availability of open-source libraries, and the proliferation of mobile computing platforms have made machine learning methods attractive for the development of field deployable, portable sensor array devices. Tsitron et al. developed a Bayesian algorithm combined with an electrochemical response model to extract concentration from mixed potential sensors in binary mixtures of ammonia and propylene.[160] Javed et al. and Ramaiyan et al. applied support vector machines and Gaussian process regression to identify 1–4 component mixtures of NO_x, ammonia, and hydrocarbons with an array of multiple mixed potential sensors (Fig. 5a).[161,162] Today, deep learning methods leveraging increased computational capability have resulted in the development of ANNs consisting of 10 s–100 s of layers. ANNs are categorized as black box methods, where the development of an explicit physical model for the sensor response is not needed. This is an advantage in multi-species analysis where the number of chemical interactions increases combinatorically with the

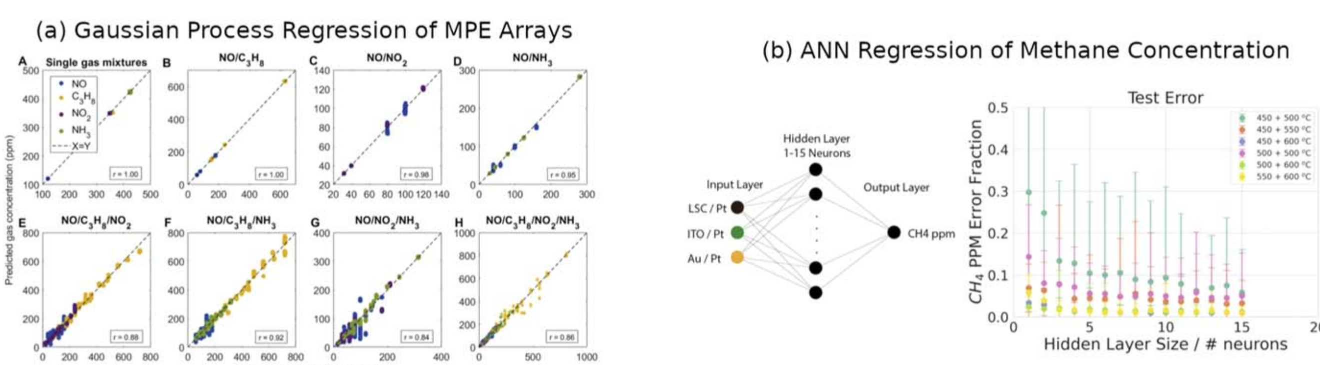

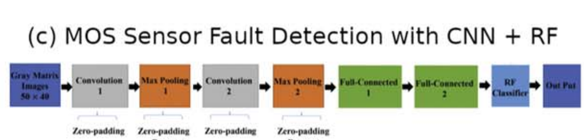

Method	Normal environment		Noisy environment	
	CNN-RF	CNN	CNN-RF	CNN
Max	100%	100%	100%	99.61%
Min	100%	99.23%	100%	98.84%
Mean	100%	99.74%	100%	98.91%

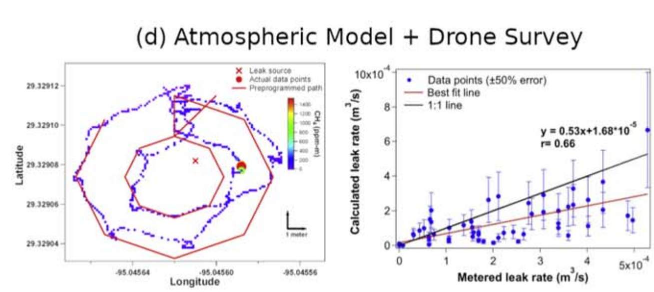

Figure 5. (a) Gaussian Process Regression for quantification of 1–4 component mixtures of NO, NO_2, C_3H_8, and NH_3. Reprinted from Ref. 161 with permission from Elsevier. (b) ANN regression of methane concentration with a four-element mixed potential sensor array. Reprinted from Ref. 16 with permission via CC-BY license. (c) Fault detection for MOS sensors with a combined convolution neural network and random forest algorithm achieving 100% detection of sensor fault. Reprinted from Ref. 165 with permission via CC-BY license. (d) Atmospheric modeling combined with drone surveying of methane concentration to predict a leak rate. Reprinted from Ref. 112 with permission via CC-BY license.

number of gas species analyzed, and it is not feasible to develop a model for each possible chemical reaction driving the sensor response. Zhang et al. benchmarked ANNs combined with other ML methods including random forest and support vector machines to show that a multi-sensor array of semiconductor sensors could accurately identify and quantify CO, H_2, and CO/H_2 mixtures.[163] An array of four metal oxide semiconducting sensors could quantify hydrogen across a concentration range of 17–3000 ppmv with a measurement error of 5.8% in the presence of hydrocarbons by use of ANNs.[164] Halley et al. demonstrated the application of ANN and ML methods to not only detect fugitive methane emissions but also to discriminate the source of that emission (Fig. 5b).[16] ML has also been applied to monitor the health of the sensor and is especially important for systems prone to drift. Sun et al. developed a convolution neural network plus random forest algorithm to detect for sensor drift in hydrogen sensitive metal oxide sensors (Fig. 5c).[165]

There is a need in emissions monitoring from a leak source not only to provide the absolute concentration of an analyte at a point but also to localize the emission to a point in space. This may be accomplished by integrating data collected from sensors spaced around a potential leak source combined with computational methods using these data. Gas dispersion models such as inverse plume methods then use the aggregate sensor data along with atmospheric conditions to predict the source of an emission (Fig. 5d).[112,132,166–169] Black box artificial neural networks without a physical atmospheric model have also successfully localized the emissions for gases from data collected with an array of sensors.[170,171] These methods have been applied for methane emissions monitoring but are expected to be applicable for hydrogen or hydrogen-methane blends as well. The increased processing power available for mobile and embedded processors has enabled the deployment of ML algorithms on IoT platforms. This enables them to perform automatic identification, quantification, and self-calibration without the need to connect to a remote server.[172–176] Mondal et al. demonstrated an ANN algorithm with an array of 6 metal oxide sensors capable of performing identification of CO, H_2, and CH_4 which fits in a 185 kb file that was deployed on a microcontroller.[177] Sensors mounted onto drones and autonomous robots could enable survey of hard to reach areas or cover large distances.[178–180] The development of ML technology integrated with edge computing and sensor arrays is a promising route for high accuracy processing of sensor data to identify, quantify, and locate emissions from hydrogen infrastructure. Physical models promise a better understandability of the results produced by the algorithm, while black box ML models are easier to develop. The main constraint with ML is obtaining large enough datasets that supervised learning can be successfully applied to. Sensors which are robust, have low drift, and high part-to-part reproducibility will be needed to minimize the amount of time expended in collecting data and performing recalibration. Field testing in relevant environments outside the laboratory is also expected to be critical to producing ML algorithms such that computations on sensor responses accurately represent the real world.

Hydrogen Sensors in Air Transportation Applications

Hydrogen has been widely used in aerospace applications for rocket propulsion and is emerging as a green fuel for civilian aircraft.[181,182] Hydrogen offers the potential for carbon-free emissions from aircraft using hydrogen turbine engines and as a fuel for electrifying aircraft primary and auxiliary systems with fuel cells. The introduction of hydrogen based technologies in aircraft systems requires new sensor technology for leaks and safety in tankage, transport, and use to support widespread adoption.[183,184] NASA Glenn Research Center and collaborators have endeavored to improve hydrogen leak detection capabilities including the development of an automated hydrogen leak detection system using micro hydrogen sensors.[155,157,185] The objective is to produce a hydrogen leak detection system which does not need oxygen or depend upon moisture to operate. Two different hydrogen detection approaches are used depending on the concentration range. The detection of low concentrations of hydrogen involves using palladium (Pd) alloy Schottky diodes on a silicon (Si) substrate. The Schottky diode structure is composed of a hydrogen-sensitive metal (Pd-alloy) deposited on an oxide (silicon dioxide) adherent to a semiconductor. This forms a Schottky diode in the form of a very thin layer (approximately 50 Å) of silicon dioxide (SiO_2). In this approach, when hydrogen reacts with the Pd-based catalytic layer, it dissociates into atomic hydrogen. The resulting atomic hydrogen is absorbed into the Pd-based layer forming a dipole layer at the Pd/SiO_2 interface causing a change in the diode electrical properties that varies with the hydrogen concentration. The hydrogen concentration can thus be measured by detecting a change in the current for a given bias voltage of the diode. The advantage of a Schottky diode sensing structure in gas sensing applications is its high sensitivity.

The detection of higher concentrations of H_2 (up to 100%) can be accomplished using a hydrogen sensitive resistor. Also based on hydrogen absorption, the resistance of the sensor changes proportionally with the amount of hydrogen in the ambient. The amount of resistance change is dependent on the hydrogen concentration in the ambient. Both the Pd-based Schottky diode and resistor do not need oxygen to quantitatively measure hydrogen. The overall approach for wide range hydrogen detection from low concentrations to 100% is to combine the characteristics of both the Schottky diode and resistor to provide a reliable response throughout the range of possible operational environments.[155]

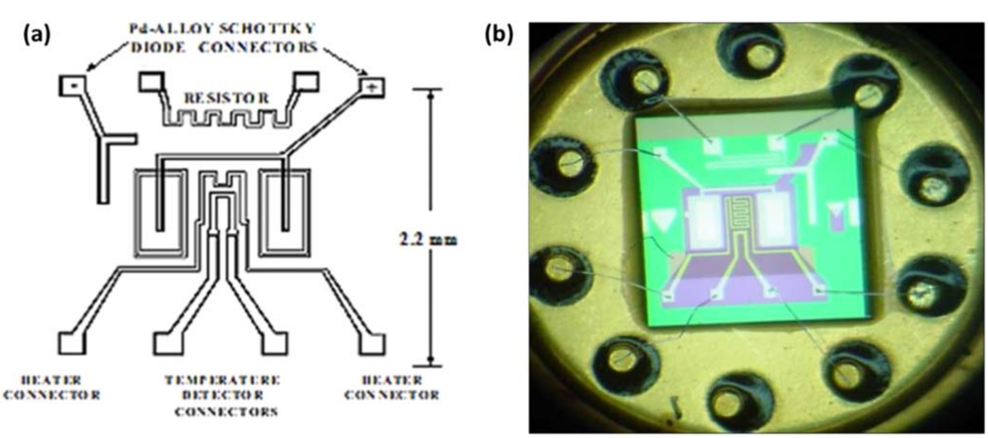

Figure 6. (a) Schematic diagram of the silicon-based hydrogen sensor. The Pd alloy Schottky diode (rectangular regions) resides symmetrically on either side of a heater and temperature detector. The Pd alloy resistor is included for high concentration measurements. (b) Picture of the packaged sensor.[155]

The design of the referenced Pd alloy sensor is shown in Fig. 6. The structure includes a Pd alloy Schottky diode and resistor, a temperature detector, and a heater all incorporated in the same chip (Fig. 6a). Also shown is a picture of the packaged sensor (Fig. 6b). The response of the Schottky diodes was determined by measuring the diode's reverse current. This Fig. 6 highlights the sensor's small size, multiple structures on the same chip, and integration with temperature control capabilities. The response of the Schottky diode and the resistor, both based on a palladium chrome (PdCr) alloy, is shown in Fig. 7.[155] The raw sensor data is shown as well as the processed and calibrated data. The processing includes filtering of signal noise. Figure 7a shows the response of a diode to hydrogen in air at low concentrations. The resistor response in air is shown in Fig. 7b to a range of high hydrogen concentrations. The calibrated response is provided to the user; the processing eliminates noise in the signal and produces a more "square wave" response while still representing the concentration present in the environment. Other data taken in inert environments (not shown), i.e., helium or nitrogen, show a diode with a slower recovery time but a more sensitive and responsive resistor.

Another approach to sensitive hydrogen detection is to replace the silicon semiconductor with a silicon carbide (SiC) semiconductor in the Schottky diode sensing structure.[186,187] The advantage of this approach is that SiC has a much wider temperature range as a semiconductor than Si allowing for use in high temperature applications, up to 600 °C, not achievable with silicon-based devices. In order to prevent reactions between the catalytic metal and the semiconductor, a controlled thickness of palladium oxide (PdO_x), is used as a barrier layer between the catalyst and the SiC. Palladium oxide is chosen as a barrier layer due to its inertness and compatibility for inclusion in the Schottky diode structure.

This palladium/palladium oxide/silicon carbide ($Pd/PdO_x/SiC$) Schottky diode sensor design is sensitive to both hydrogen and, at higher temperatures, hydrocarbons (including methane depending on the sensor temperature).[188] Figure 8 shows the output current of $Pd/PdO_x/SiC$ sensor biased at 0.45 V at 180 °C during exposure to hydrogen concentrations in nitrogen at a concentration range below 1.25 ppmv. The sensor at these higher temperatures is capable of sensing H_2 as low as 0.25 ppmv at this bias voltage. Such sensitivity was not seen at lower temperatures and so this data demonstrated tuning the sensor response using temperature control.[126] Overall, this sensor has demonstrated a broad range of detection capability and has been applied in multiple applications beyond leak detection, e.g., emissions monitoring or fire detection.[189,190]

Implementation of hydrogen sensor systems for aircraft applications requires certification and design considerations which differ from ground infrastructure.[191] Hydrogen sensors and associated electronics for aircraft applications must be capable of operating in reduced and oxygen-free environments during flight, operate at

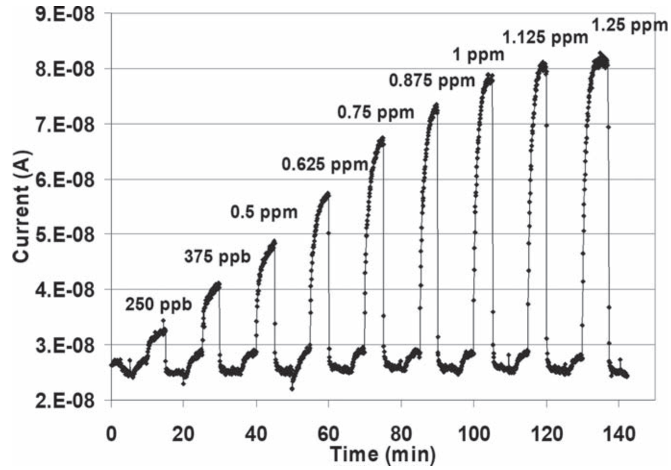

Figure 8. Plot of output current of the $Pd/PdO_x/SiC$ sensor biased at 0.45 V at 180 °C. Sensor was exposed to different hydrogen concentrations in nitrogen with exposure to air and then nitrogen in between each hydrogen exposure. This data shows that the sensor can be optimized to detect hydrogen concentration as low as 250 ppbv.[189]

maximum temperatures well below potential hydrogen ignition temperatures, and be capable of flight safety certification. hydrogen sensor systems require electronics and packaging. The typical safety system certification requirements for aircraft sensor systems include compliance with RTCA DO-254 Airborne Electronic Hardware Design Assurance, RTCA DO-178C Software Considerations in Airborne Systems and Equipment Certification, and RTCA DO-160G Environmental Conditions and Test Procedures for Airborne Equipment. Additionally, new technical standard guidelines are currently under development for aircraft and airports which may drive technology requirements for aircraft hydrogen sensors.[192]

Review of Currently Available Commercial Sensors for H_2, CH_4, and NH_3

This section is focused on existing commercial and near-term sensors for the target gases hydrogen, ammonia, and methane. The near-term sensors are included since they have possibilities to impact the commercial markets with only minor developments or specific deployment options that can make them immediately useful. The call for smart measurements, automated systems, and intelligent feedback in every aspect of life result in an increasing demand for all types of gas sensors. This is reflected by the projections for the commercial gas sensor market which had a value of \$1.4 billion in 2022 and is projected to increase to \$2.1 billion by 2027.[193]

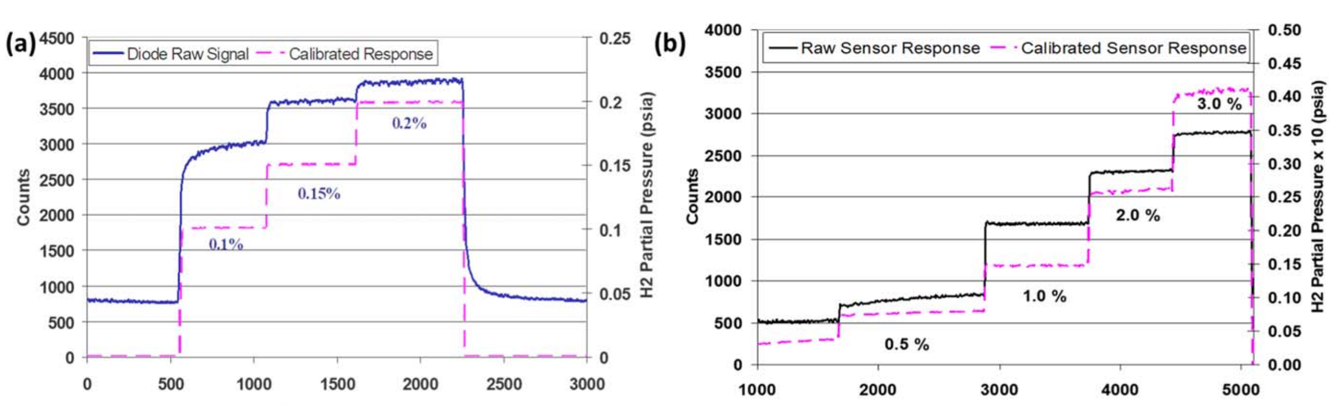

Figure 7. Pd Alloy based (a) Schottky diode and (b) resistor response to hydrogen in air. Both the raw signal and calibrated response are shown. The responses of the two sensor types are complementary spanning the hydrogen concentration range from low concentrations to 100%.[155]

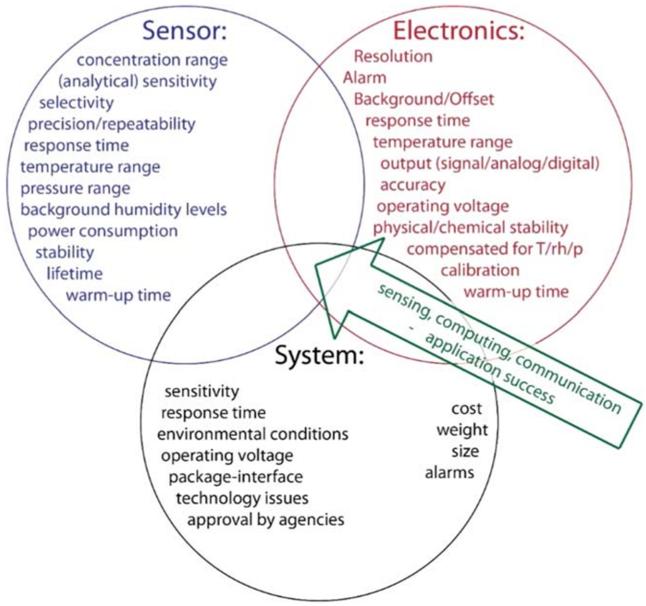

Figure 9. Overview of the different requirements for the three components of a modern gas sensor that will influence the choice for a specific commercial application.

Additionally, the use of natural gas and hydrogen as an energy source is growing rapidly while at the same time our understanding of the role that gases like methane and hydrogen play in climate change increases. Another environmentally relevant gas is ammonia, a toxic gas, and it is also relevant to the safe emergence of the hydrogen economy. The increasing use of hydrogen and methane as an energy source, as well as the increasing need for fertilizers to feed the world's population are foundational for the increasing need in commercial monitoring methods to detect gas leaks and monitor these specific toxic, environmentally significant, and explosive gases.

The basic sensing element must meet specifications that allow a successful application. One must know the requirements imposed by the application in order to either develop a successful sensor or to select a commercial sensor for field use. The system or package has an additional requirement that the entire sensor package has to be supported and have a reliable supply chain. Commercially available sensor solutions are based on a variety of technologies. This includes electrochemical, chemiresistive, Shottky diodes devices, optical sensors using absorptive or emissive techniques, thermal sensors based on thermal conductivity or catalytic combustion, and mechanical sensors based on piezoelectric films. Each technology has certain advantages and disadvantages, as well as application cases where one of the technologies is more favored than another. The choice for a specific technology is often based on the requirements that can be achieved with the entire sensor system and packaging. Specifications for commercial sensors are typically presented in a table to enable easy selection of the sensor for a given application. It implies that one knows a lot about the condition of deployment of the sensors. The specification for the commercial sensor must include the performance of sensor, electronics, and system with packaging. Commercial applications are generally examined differently than sensor investigations and the final performance specifications are driven by the system and not necessarily those of the discreet sensor element within. This is easily seen wherein the package limits the gas access and thereby determines the measurement response time no matter how fast the sensor element may be. Within this cadre of specifications (Fig. 9), one considers the measurement to be made, the situation in which these are made and all the variables therein. These complex considerations provide focus for development as well as applicability of commercial sensors. Figure 9 provides an overview of the different requirements for the sensor, the electronics and the system that need to be met by the sensor of choice for a specific application. There is also a disciplined tiered approach to the evaluation of a sensor towards satisfying a specific commercial application.[194] It is reasonable to assume that the sensor signal has an error due to fluctuations in any variable that changes the signal (output) of the sensor. These are typically modeled as a simple term that adds or subtracts to the overall signal vs concentration equation.

This section of the review provides a brief introduction into each technology including references for more detailed explanations of the working principles, as well as tables with commercially available sensors. It should be kept in mind that there are more sensor manufacturers out there than will be listed in Tables III–VIII. These tables are just intended as a short glimpse into the vast variety of commercially available sensors, and we apologize to anyone who is not included in this review at this time. Whenever possible, the tables presented includes information on concentration range, power consumption, cross sensitivities, expected lifetime and the link to the manufacturer data sheet/url.

Electrochemical sensors.—The working principles of electrochemical sensors are discussed in Sensors for the Hydrogen Economy section and will not be discussed again at this point. Electrochemical gas sensors can be used for a broad range of gases and can therefore be used in hydrogen, methane, and ammonia detection and monitoring applications. The advantages of electrochemical gas sensors are their relatively small size, low cost, and low power consumption allowing for designing portable or fixed site instrumentation as well as disposables. Electrochemical sensors often have high sensitivity coupled with selectivity but can be inadequate for some field applications even today because of the stability of the electrolyte or package in different conditions, especially humidity and temperature. In many commercial electrochemical gas sensors, the electrolyte is an aqueous acidic solution which swells in high humidity due to water uptake but can also dry out in low humidity resulting in severely changing volumes and impedances of the electrolyte. High-temperature cells avoid aqueous electrolytes but also have limitations. Swelling of the liquid electrolytes is typically handled with a built-in cavity to accommodate the electrolyte volume changes. Despite the cavity, electrolyte leaking can occur which can result in a loss of sensor performance due to a loss of electrolyte but a good package can have lifetimes in excess of 10 years. The operational temperature range of electrochemical sensors is also limited due to the physical properties of the electrolyte and package. To be more exact, if the electrolyte is an aqueous solution, the external temperature of the sensor is limited to above the freezing point of the electrolyte and to temperatures low enough so that the electrolyte will not evaporate. Current research in the field of electrochemical sensors involve investigations of both aqueous[195] and non-aqueous electrolytes like room temperature ionic liquids (RTILs) which enable a wider temperature range as well as can limit the water uptake due to inherent hydrophobicity.[196,197] While no or few devices implementing RTILs are currently commercially available, the progress in this field is promising. Despite the disadvantages just discussed, the versatility, low cost, low power, small size and reliability of electrochemical gas sensors make them extremely interesting for a broad range of applications which results in a high number of commercially available sensors for hydrogen and ammonia (Table III). Despite research papers on amperometric methane sensors[198] since 1983, there are no commercial amperometric sensors for this gas and therefore Table III focuses on presenting sensors for hydrogen and ammonia.

Chemiresistive gas sensors.—Many commercially available sensors for methane are based on metal oxide semiconductors (MOS), often loaded with noble metals, other MOSs, or with carbon nanotubes (CNTs).[224–226] In the early 1960s, it was discovered that

Table III. Overview of several commercially available electrochemical gas sensors showing their concentration ranges, power consumptions, cross sensitivities and lifetime.

Gas	Manufacturer	Concentration range	Power consumption	Cross sensitivities	Lifetime	References
H_2	Alphasense	0–2000 ppm		CO, NO_2, Cl_2, NO, SO_2, H_2S, C_2H_4, NH_3, CO_2	2 years	199
	Control Instruments Corporation	0–2000 ppm			2 years	200
	Critical Environment Technologies	0–2000 ppm		NH_3, CO, Cl_2, ethylene, ethylene oxide, formaldehyde, H_2, HF, H_2S, NO, NO_2, O_2, O_3, SO_2	2–3 years	201
	Det-Tronics	0–1000 ppm	0.8 W	H_2S, NH_3, O_2, CO, SO_2, Cl_2, NO_2	18 months	202
	Drägerwerk AG	15–3000 ppm		Toxic gases		203
	Euro-Gas management services	0–4%		CO, ethylene	2 years	204
	Teledyn Detcon	0–100 ppm	750 mW		2 years	205
		0–2000 ppm	2 W	O_2, H_2S, NH_3, CO, NO, NO_2, SO_2, Cl_2, HCl, HCN	2 years	206
	Industrial Scientific	0–2000 ppm		CO, H_2S, SO_2	>5 years	207
	Membrapor	0–40000 ppm		CO	2 years	208
	International Gas Detectors	0–1000 ppm		O_2, CO, SO_2, H_2S, NH_3	>2 years	209
	Safety Systems Technology	0–5000 ppm		H_2S, CO, Cl_2, ethylene oxide, NH_3, HCl, HCN, H_2O_2, NO, NO_2, PH_3, SO_2	1 year	210
	Sensitron	0–3000 ppm	5.4 W	O_2, CO, H_2S, NO, NH_3	2–3 years	211
	SGX Sensortech	0–1000 ppm		CO, NO_2, ethene	2 years	212
	Zhengzhou Winsen Electronics Technology	0–1000 ppm		CO, O_2, H_2S, NO_2, HCl, NH_3, PH_3, SO_2, O_3, Cl_2, HF	2 years	213
NH_3	AlphaSense	0–100 ppm		H_2S, NO_2, Cl_2, NO, CO, H_2, ethene	>2 years	214
	Drägerwerk AG	15–3000 ppm		Toxic gases, H_2, O_2		203
	Eikon OÜ	0–1000 ppm	<2 W	None listed	>2 years	215
	Figaro Engineering	0–5000 ppm		H_2S, NO_2, SO_2	>2 years	216
	Teledyne	0–1000 ppm	2 W	O_2, H_2S, H_2, CO, NO, NO_2, SO_2, Cl_2, HCl, HCN	2 years	206
		0–100 ppm	750 mW	Acetylene, arsine, Br_2, butadiene, CO, Cl_2, ClO_2, diborane, ethanol, ethylene, ethylene oxide, F_2, formaldehyde, germane, H_2, HCl, HCN, HF, H_2S, methanol, methyl mercaptan, nitric oxide, NO_2, O_2, O_3, phosphine, silane, SO_2	2 years	217
	Honeywell	0–1000 ppm		None listed	3–5 years	218
	Industrial Scientific	0–500 ppm		None listed	>5 years	207
	LogiDataTech	0–100 ppm		Cl_2, CO, H_2S, NO_2, O_2, SO_2		219
	Membrapor	0–10000 ppm		H_2S, NO, NO_2, SO_2	2 years	220
	Nemoto Sensor Engineering	0–5000 ppm		H_2, H_2S, SO_2, NO_2	2 years	221
	International Gas Detectors	0–100 ppm		O_2, CO, H_2, H_2S, SO_2	>2 years	222
	Safety Systems Technology	0–5000 ppm		H_2S, CO, Cl_2, ethylene oxide, H_2, HCl, HCN, H_2O_2, NO, NO_2, PH_3, SO_2	1 year	210
	Sensitron	0–5000 ppm	5.4 W	O_2, CO, H_2S, NO, H_2	2–3 years	211

Table III. (Continued).

Gas	Manufacturer	Concentration range	Power consumption	Cross sensitivities	Lifetime	References
	Process Sensing Technology	0–1000 ppm		None listed		222
	SGX Sensortech	0–1000 ppm	1.3 W	H_2S, NO_2, SO_2	>2 years	223
	Zhengzhou Winsen Electronics Technology	0–100 ppm		CO, O_2, H_2S, NO_2, HCl, H_2, PH_3, SO_2, O_3, Cl_2, HF	2 years	213

ZnO changed resistance depending on the composition of the atmosphere.[227] This was followed by the development of the first commercial MOS-based chemiresistive sensor in the late 60's by Naoyoshi Taguchi who developed a low-cost sensor that was installed easily enough to be a bestseller for people that used natural gas for cooking (mostly methane). The commercialization of this device significantly reduced the number of domestic gas explosions in Japan and improved safety.[228] The sensor was based on SnO_2 loaded with PdO_x and was the initiator for a surge in research on chemiresistive gas sensors.

MOS based chemiresistive sensors are in general considered to be easily processible, low-cost, robust, and easily miniaturizable and can be a MEMS (micro-electromechanical system) compatible technology. The sensors usually consist of a heating element which ensures the optimal operating temperature of the sensing layer deposited on 2 or more electrodes that are used for the electrical readout of impedance. Gas sensing with chemiresistive gas sensors can be separated by the nature of the reaction of a target gas at the surface of the sensing material, and the transduction mechanism which is the translation of this reaction into a readable sensor response. In the case of chemiresistive sensors, surface reactions that result in a charge transfer are translated into a change in resistance. A detailed explanation of the chemical reaction and signal transduction mechanisms can be found in Refs. 229–231. Sensors based on pristine MOS materials often suffer from a lack of selectivity, strong cross-interferences with especially humidity but also other gases, in addition to requiring high operation temperatures (between 200 °C–600 °C) which results in a relatively high-power consumption. It was found that the implementation of heterostructures can result in both a reduction of the operation temperature and/or increase of the sensor's selectivity and sensitivity to certain target gases through chemical or electronic sensitization effects. While the underlying sensitization mechanisms are now fairly well understood, it is still difficult to predict how a sensor based on a heterostructure will react to a target gas since the structure-function relationships are not yet fully understood. The sensor mechanisms and their current understanding are discussed in detail in the literature.[232–234]

Most commercially available chemiresistive sensors contain heterostructures made from MOSs as base material surface modified with noble metals or other metal oxides. They can be purchased for several target gases. This includes the gases of interest in this review (CH_4, H_2 and NH_3) but also other gases like CO, CO_2, VOCs, O_3 and NO_2. Among the most well-known companies marketing MOS-based sensors are Figaro Engineering Inc. (Japan), Alphasense Sensors (United Kingdom), Sensirion AG (Switzerland) and Honeywell Analytics, Inc. (United States).[235] There are numerous other companies that produce and market MOS-based sensors. Table IV lists some of those companies and their commercially available sensors for methane, ammonia and hydrogen.

Optical sensors.—The fundamentals of optical sensors (UV to IR) can be explained with the help of the Jablonski diagram which shows the electronic states in addition to the vibrational levels that are characteristic for each target molecule.[248] Optical sensing can result when light is measured after interacting (absorption or emission) with these energy levels within the target molecule. This mechanism can often result in very high selectivity by selection of the specific wavelength of light to match the molecular energy transitions for the specific gas. Many recent reviews on this topic are available in the literature.[52,249–253] Sensors using different regions of the electromagnetic spectrum are available today for many gases. The different electromagnetic regions are: UV (200–400 nm), near-IR (700 nm–2.5 μm) or mid-IR (2.5–14 μm) and while UV radiation interacts to cause electronic transitions, IR radiation interacts with molecular vibrational and rotational states (mid-IR: fundamental; near-IR: overtone and combination).

Optical gas sensors can either be absorption-based or emission-based. Emission-based optical sensors include sensors that are based on chemiluminescence and fluorescence. Chemiluminescence-based sensors are often used for the detection of nitrogen oxides since excited NO_2 releases light with a characteristic wavelength when it relaxes. Fluorescence-based sensors can be used for the detection of sulfur-containing compounds like SO_2 and are similar to the just mentioned chemiluminescence-based sensors, the gas absorbs light and ends up in an excited state. Upon relaxation, the molecules release light of a characteristic energy that can be measured. The differences between chemiluminescence and fluorescence are discussed elsewhere.[248] Both just mentioned technologies are usually packaged into stationary instruments (larger than what is considered a simple sensor device) due to the required equipment for these methods. The most well-known UV-based optical sensors that are available as hand-held devices are photoionization detectors (PIDs). They contain a UV radiation source that ionizes gases if the chemicals have ionization energies lower than or equal to the energy of the UV radiation produced by the lamp. The ions are then counted by neutralization at an electrode resulting in a current. The more ionizable gasses that are present, more ions that are produced, resulting in a larger current signal. While ionization energies are characteristic for each molecule, PIDs are not considered to be selective gas sensors since the UV radiation source will ionize everything that can be ionized at that lamp energy level. This will result in a measurable current that directly correlates to the concentration of total ionized gas. While PIDs lack selectivity, they are capable of measurement over a wide concentration range and are capable of detecting gases like ammonia which is often difficult to detect with other technologies.

Absorption-based optical gas sensors are used significantly more often than emission-based ones for the gases of interest. They usually consist of a light source, a gas cell, and a detector. The exact design of the absorption-based optical sensor varies greatly in size and power consumption. The most common optical gas sensors are non-dispersive infrared (NDIR) sensors which are often used for the detection of CO_2, but with the help of filters can be used for virtually any gas that is IR active including methane and ammonia. Diatomic molecules like H_2 are not IR active. With recent developments, it is possible to build compact devices with dimensions of approximately $16 \times 20\,mm^2$ for gases with high excitation coefficients. They contain a micro bulb as a light source, a gold-coated reflective light path, and an integrated detector with at least two filtered detection channels. The emission of the micro bulb is directed through the two channels—a sample channel and a reference channel. Both channels are equipped with carefully selected filters to improve the selective detection of a specific gas by filtering any radiation outside the required energy range. When the beam hits a gas, the gas will absorb certain energies and will get excited. The detector will measure the energy loss in the vibrating molecules (in case of an NDIR sensor) due to absorption by the gas vs the non-absorbing reference light beam. The amount of absorbed energy is directly correlated to the concentration of the gas via the Beer–Lambert law. The reference channel ensures that changes in the background will be eliminated from the resulting spectrum. It should be noted that diatomic molecules like H_2, N_2 or O_2 are not IR active and are not detected with simple IR sensors, but CH_4 and NH_3 are good candidates for IR sensors. Among the key players on the NDIR market are Honeywell Analytics (United States), Senseair AB (Sweden) and S+S Regeltechnik (Germany),[254] although not for the gases discussed herein. The overall NDIR market had a value of \$0.7 billion in 2022 and is projected to grow to \$1 billion by 2027.[254]

Open-path IR sensors have been used in the petrochemical and related industries for the detection of methane and other hydrocarbons. The sensors are called "open-path" because the IR beam passes through open space between the transmitter (radiation source) and the receiver (detector) unit. This results in a measurement of the sum of all gases present in the path and usually has the unit ppm.m or LEL.m.[255] The path lengths can be as long as several hundred meters but can also be significantly shorter. An example for an open-path device would be sensors using differential optical absorption spectroscopy (DOAS). They are equipped with a high-power Xenon

Table IV. Overview of several commercially available chemiresistive gas sensors showing their concentration ranges, power consumptions, cross sensitivities and lifetime as reported.

Gas	Manufacturer	Concentration Range	Power consumption	Cross sensitivities	Lifetime	References
H_2	ScioSense	0–1000 ppm		Ethanol, acetone, CO, toluene		236
	Duoyi	>5 ppm		Methane, ethane, propane, butane, acetone, ethane, ammonia, naphthalene		237
	Envin Scientific Limited	1–150 ppm	40 W	CO, CH_4		238
	Evikon OÜ	0–100% LEL	<2 W	CH_4, acetylene, propane, butane, hexane, octane	>5 years	239
	Nissha Fis Inc.	10–10000 ppm	120–400 mW	CH_4, iso-butane, ethanol, propane, CO		240
	SGX Sensortech	1–1000 ppm	200 mW	Ethanol, H_2, propane, iso-butane		241
CH_4	Evikon OÜ	0–100% LEL	<2 W	None listed	>5 years	242
	Figaro Engineering	1–25% LEL	10–280 mW	Iso-butane, propane, H_2, ethanol, CO		243
	NISSHA FIS Inc.	100–10000 ppm	34–400 mW	H_2, iso-butane, ethanol, CO, propane,		244
	LogiDataTech	0–50% LEL		VOCs		245
	Zhengzhou Winsen Electronics Technology	300–10000 ppm	<1 W	Alcohol, butane, H_2O	10 years	246
	SGX Sensortech	>1000 ppm	200 mW	CO, ethanol, H_2, NH_3		247
NH_3	SGX Sensortech	1–500 ppm	200 mW	Ethanol, H_2, propane, iso-butane		241

lamp which can cover path lengths of up to 1 km or more and are often used for gases that are not IR active but relevant for air quality monitoring. DOAS sensors are also often used to monitor emissions in ventilation ducts.[255]

Differential absorption light detection and ranging (LIDAR) is a laser-based optical gas detection method that is capable of measuring gas concentrations down to low-ppb concentrations at a remote point. It is a very powerful tool, but also a very costly one that requires a lot of space (often housed in a van or even bigger vehicles). The high-power laser is operated at two different wavelengths—one which the gas of interest absorbs and the other at a wavelength the target gas does not absorb. Based on the differences in the signal detected at the two different wavelengths, the concentration of the target at the remote point can be estimated. The distance of the remote point can be tuned with the help of the frequency one switches between the two different wavelengths. By integrating both an IR and a UV laser, the number of gases that can be measured increases, however, the instrument becomes also more expensive. Devices like these are often used to monitor leaks from processing or storage facilities, greenhouse gas emissions from landfill sites, or emissions from petrochemical plants. Table V lists some of the companies and their commercially available optical gas sensors for methane, ammonia and hydrogen. Optical detection can even be performed from the International Space Station by looking at specific wavelengths of light emitted by the earth from its surface.

Thermal sensors.—There are different types of thermal sensors. The most common type is the pellistor-type catalytic sensor, often called a combustible gas sensors (CGS). They are generally used for the detection of combustible gases like volatile organic compounds. Since the combustible gas is oxidized in this process, there must be a minimum O_2 level of 5–10 vol% in the environment, otherwise the combustible gas will only be partially burnt resulting in false readouts and the catalytic sensor will get covered in soot. Pellistor-type catalytic sensors often consist of two oxide beads covering a fine Pt wire. One of the beads is coated with a catalyst, the other one is unreactive to combustible gases up until the lower explosion limit (LEL) is reached. The latter is used as the reference bead. When a combustible gas gets in contact with the catalytically activated bead, the gas is burned. This process is exothermic and results in an increase in temperature of the active bead. The temperature change can be detected as a change in resistance of the fine Pt wire of the active bead relative to the resistance of the wire in the reference bead. This change in resistance is directly related to the concentration of the combustible gas. Pellistor-type sensors should not be used for concentrations above the lower explosion limit (LEL) since a fall-off of the signal will be observed at higher concentrations causing possibly fatal false negative responses. The company MSA has a slight variation in the beads: both beads are platinum wires which is a catalytically active material, however, the reference bead is coated with glass resulting in an inert bead while the other bead is still catalytically active.[270] Coating the reference bead with the inert glass layer is reported to improve baseline stability compared to the other designs.

The other type of thermal gas sensor often found are thermal conductivity detectors (TCD). Their advantage is their ability to measure H_2 from 0–100% and their ability to measure any gas with differing thermal conductivities. Pellistor-type sensors can only detect combustible gases but cannot differentiate gases with differing thermal conductivities. In contrast, thermal conductivity-based gas sensors are built very similarly to pellistor-type sensors but differ in the signal of the TCD which is now the change in thermal conductivity of the gas causing a change in temperature thus resulting in a change in resistance of the TCD filament or a change in the power required to keep the TCD elements at constant temperature. While pellistor-type sensors are limited to the detection of combustible gases, thermal conductivity sensors have a significantly broader range of gases that can be measured since virtually every gas has a differing thermal conductivity. While this is a benefit most of the time, the fact that TCDs require the measured gas to have a significantly different thermal conductivity compared to the background results in a different set of limitations. For example, it is difficult to measure O_2 in a N_2 background since the two gases have very similar thermal conductivities. H_2 or CH_4 in air, however, can be easily measured over the full 0–100% concentration range and hydrogen is especially sensitive since its thermal conductivity is about 10 times that of background air. TCDs also become more sensitive as they are miniaturized and can respond very fast (microseconds) when miniaturized.[53,271,272]

To summarize, thermal sensors are in general not selective for gases. Pellistor-type sensors cannot distinguish between two different combustible gases. Similarly, TCDs need a defined background to give reliable concentration measurements of certain gases. Additionally, thermal sensors are susceptible to interferences with other gases that could damage the sensor preventing the recovery of the sensor by covering it in soot or contaminating the beads. However, in contrast to most other sensor technologies, thermal sensors are less sensitive to humidity changes as well as external temperature variations, can last a very long time, and can be used for rapid detection and alarm situations. Table VI lists some of the commercially available thermal gas sensor manufacturers for methane, ammonia and hydrogen.

Piezoelectric sensors.—Piezoelectric sensors are the oldest and simplest acoustic gas sensors and have been used since 1964.[293] They detect changes in the properties of acoustic waves due to adsorption at the surface or absorption in the bulk of a piezoelectric material. One of the detected properties is the resonance frequency which will change in dependence of the deformation of the crystalline sensing element, and therefore can be used to indicate the concentration of the target gases hydrogen, methane, or ammonia. There are multiple causes for the piezoelectric materials resonance frequency changes: (1) the accumulation of mass on the surface of the crystal changes the resonance frequency; (2) the catalytic oxidation of the target gas on the surface of the crystal increases the temperature and causes an increase in the resonance frequency of the crystal.[294] Various noble metal catalyst coatings have been tested and a Pt–Ir film resulted in the best performance;[295] (3) the change in target gas concentration (e.g., H_2, CH_4, or NH_3) results in a shift of the sound–resonance state of the piezoelectric element. A piezoelectric–sound–resonance–cavity (PSRC) sensor, for example, utilizes this mechanism.[296] The sensor has a sensitivity limit of 8 ppmv, a broad operational concentration range and a fast response time. Moreover, some surface acoustic wave (SAW) gas sensors utilize the advantage of the sensitive material's piezoelectric effect, whose frequency shifts due to the adsorption of analyte gas molecules; the electrical conductivity changes when the sensing layer (e.g., the palladium or copper phthalocyanine layer) absorbs the target gas resulting in a detectable change in the frequency.

The most commonly used piezoelectric substrate material is $LiNbO_3$, although $LiTaO_3$[297] has been used as well. $LiNbO_3$ or $LiTaO_3$ are coated onto the piezoelectric substrate's gas selective layer between the two sets of interdigitated transducers (IDTs). Multiple sensing layers (e.g. Pd/WO_3 bilayer), or tube structures are used to improve the performance and sensitivity.

Hydrogen, methane, and ammonia have higher sound velocities compared to air as shown in Table VII. This difference can be used for their concentration measurement in gas mixtures. Several sound-velocity based gas sensors have been developed. Wan et al. generated acoustic waves in a gaseous medium by laser irradiation of a chemically inert sensitizer and measured the propagation time of these waves as a function of the hydrogen concentration.[298] More recently, Vyas et al. described such a sensor using a pulse-receiver to generate the acoustic wave and to detect the echo.[299] Variations in temperature also affect the wave's velocity and therefore must be compensated for.

Piezoelectric based sensors have the potential to detect hydrogen, methane, and ammonia over a wide concentration range spanning

Table V. **Overview of several commercially available optical gas sensors showing their concentration ranges, power consumptions, cross sensitivities, and lifetime.**

Gas	Manufacturer	Concentration range	Power consumption	Cross sensitivities	Lifetime	References
H_2	Materion GmbH	0.1–100%	960 mW	None listed	>2 years	256
CH_4	AlphaSense	0–100%	300 mW	None listed	>3 years	257
	Drägerwerk AG	None listed	2.2 W	None listed		258
	Teledyne Gas & Flame Detection	0–100%	3.5 W	carbohydrates	5 years	259
		0–20% LEL	3.5 W	carbohydrates	5 years	260
		>0.15 lEL.m	6 W	carbohydrates	10 years	261
	Honeywell	0–100% LEL	<4.5 W	Carbohydrates		262
	Industrial Scientific	0.1–100%		carbohydrates		207
	MSA—the safety company	0–5 lEL.m	10–12 W	H_2S, ethylene, NH_3, CO_2, HCl, HF	>5 years	263
	Nova Analytical Systems	0–100%		hydrocarbons		264
	Process Sensor Technology	0–500 ppm 0–100%	<480 mW	hydrocarbons		222
	Fer Strumenti	0–50 ppm	70 W	CO, CO_2, NO, SO_2, HCl, NH_3, O_2		265
	SGX Sensortech	0–100%	180 mW	Hydrocarbons, humidity	>10 years	266
NH_3	Ion Science	0–10000 ppm	10–12 W	H_2S, ethylene, CH_4, CO_2, HCl, HF	>5 years	267
	Fer Strumenti	0–50 ppm	70 W	CO, CO_2, NO, SO_2, HCl, CH_4, O_2		265
	SPECTREX	0–500 ppm.m	<6.4 W	None listed		268
	MSA—the safety company	0–5 lEL.m	10–12 W	H_2S, ethylene, CH_4, CO_2, HCl, HF	>5 years	263
	Honeywell	0.01–1000 ppm	<0.6 W	Benzene, NH_3, vinyl chloride, toluene, phenol, acetone, xylene	1–2 years	269

Table VI. Overview of several commercially available thermal gas sensors showing their concentration ranges, power consumptions, cross sensitivities and lifetime.

Gas	Manufacturer	Concentration range	Power consumption	Cross sensitivities	Lifetime	References
H_2	ADEV Italy	0–3%	45 W	Combustible gases		273
	AirTest	0–5%	6 W	Butane, LNG, CH_4	3 years	274
	Analox Group	0–4%		None listed		275
	Crowcon	0–2000 ppm		None listed	5 years	276
	Det-Tronics	0–100% LEL		Combustible gases	3–5 years	277
	Dräger	10–100% LEL	<3.5 W	combustible gases		278
	Evikon OÜ	0–100% LEL	<2 W	CH_4, acetylene, propane, butane, hexane, octane	>5 years	279
	Figaro Engineering	0–100% LEL	525 mW	Butane, propane, CH_4		280
	General Tools	>5 ppm		CH_4, iso-butane, ethanol, ethylene, tetrachloroethylene, dimethyl sulfide, toluene, formaldehyde, diethyl ether, ethyl acetate, dichloromethane, ammonia	3 years	281
	Kane	<20 ppm		CH_4, propane, acetone, alcohol, ammonia, benzene, butane, ethylene, naphthalene		282
	MSA—the safety company	0–100% LEL		Combustible gases	5 years	283
	City Technology Engineering	0–100% LEL	295 mW	CH_4, ethane, propane, butane, pentane, hexane, CO	12 months	284
	LogiDataTech	0–100% LEL		CH_4, CH_x, LPG, formaldehyde		285
	Kebaili	0–100% LEL	30 mW	None listed		286
	Nemoto Sensor Engineering	0–100% LEL	<440 mW	None listed	>5 years	287
	Posifa Technologies Inc.	<4%	40 mW	CH_4, humidity		288
	Process Sensor Technology	0–100% LEL		Hydrocarbons including CH_4		222
	SGX Sensortech	0–60% LEL	255 mW	Combustible gases	1 year	289
	Xensor	100 ppm–100%	100 mW	Non-selective		290
CH_4	Dräger	10–100% LEL	<3.5 W	combustible gases		278
	Figaro Engineering	0–100% LEL	525 mW	Iso-butane, propane, H_2		280
	Teledyne	0–100% LEL	2 W	Combustible gases		291
	City Technology Engineering	0–100% LEL	295 mW	H_2, ethane, propane, butane, pentane, hexane, CO	>5 years	284
		0–100% LEL	295 mW	H_2	12 months	284
	Industrial Scientific	0–5%		Combustible gases		207
	LogiDataTech	0–100% LEL		H_2, CH_x, LPG, formaldehyde		285
	Safety Systems Technology	0%-100% LEL		Combustible gases	5 years	292
	Sensitron	0–100% LEL	5.4 W	Combustible gases	4–5 years	211
	Process Sensor Technology	0–100% LEL		Hydrocarbons, H_2		222
	SGX Sensortech	0–60% LEL	150 mW	Combustible gases	1 year	289

Table VII. Sound Velocity of hydrogen, methane, ammonia, and Air.[300]

Gas	m/s
Hydrogen (27 °C)	1320
Methane (41 °C)	466
Ammonia (30 °C)	440
Air (20 °C)	343

from ppm level to 100%, with rapid response times and relatively low power consumption. However, their long-term stability needs to be improved and their sensitivity to temperature and interference from other gases need to be considered and compensated by using a reference element.[295] Due to their high mass sensitivity, piezoelectric sensors are very vulnerable to interferences from coexisting gases, including humidity. Table VIII gives an overview over several commercially available piezoelectric gas sensors.

Other technologies.—There are technologies that are less common than the above-mentioned technologies but very powerful. Gravimetric sensors have shown some success in recent years. The most common gravimetric sensors are probably surface acoustic wave gas sensors, where an input interdigitated transducer (IDT) is used to induce an acoustic wave that propagates through a piezoelectric substrate to an output IDT. When a gas adsorbs on the piezoelectric substrate in between the two IDTs, the properties of the acoustic wave are influenced and the change in properties will be detected at the output IDT. Among other things, the detected change depends on the mass of the adsorbed molecule, therefore, SAW gas sensors are considered to be gravimetric sensors. By depositing a second material in between the two IDTs, the sensor's selectivity can be changed to favor one gas adsorbate or another.

The company H2scan commercialized a sensor based on a diode structure and resistive film that changed electrical properties upon exposure to hydrogen (developed originally at Sandia National Lab)[307] and has developed a highly selective gas sensor for hydrogen. This commercial sensor uses an approach similar to that described in Hydrogen Sensors in Air Transportation Applications section, and it uses a Pd-Ni alloy that first splits H_2 into hydrogen atoms on the Pd particles and then reversibly absorbs the atoms into the material. The selectivity is based on the thermodynamics of the different reactions on the Pd particles and apart from the reaction with hydrogen, the approach is quite selective since no other reactions occur at a relevant rate.[308]

An overview of acoustic and resistive based hydrogen gas sensors is given in Table IX. Det-Tronic markets an acoustic gas sensor that is equipped with a microphone that is capable to detect gas leaks by analyzing the sound generated by a pressurized leak. The detected signal depends on pressure, leak rate, gas viscosity and distance from the acoustic sensor. An advantage of this acoustic technology over other technologies is the fact that wind has no significant influence on the detected signal. With other technologies, wind can carry away the gas from the detector resulting in delayed alarms or false readings of lower concentrations.[309] The disadvantage of this technology is that it is not selective for a specific gas. It detects sounds of leaks not gases.

Riken Keiki Co., Ltd produces a device that combines an optical sensor with an acoustic sensor.[310] The measured value is calorific which means that gases without heat content like N_2, CO_2 and O_2 will not be detected. The device is used in multiple industries like oil refining, steel industry, laboratories, gas companies and turbine manufacturing. Commercial gas sensors based on a magnetic working principle utilize the change in one of the magnetic properties of active materials due to exposure to the target gas molecules. These properties include: (1) the Hall effect, (2) magnetization, (3) spin change effects, (4) the ferromagnetic resonance (FMR) effect, (5) the magneto-optical Kerr effect (MOKE), (6) the magneto-plasmonic effect, (7) magneto-static wave oscillation effect, and (8) the magneto-static spin-wave (MSW) effect. When the Hall-effect is the property of interest for the detection of hydrogen, adsorbed species of H_2 and O_2 at the surface of SnO_2 nanowires react with each other and change the electron density at the surface of the SnO_2 nanowires, resulting in a change in Hall voltage.[311] In the Magneto-optic Kerr effect (MOKE) case, the change in the polarization and intensity of reflected light from a magnetized surface is measured. This type of magnetic gas sensing uses a very small magnetic field (~50 Oe) at room temperature. The MOKE technique offers great advantages due to its high surface-sensitive properties and the signal is not affected by the paramagnetic and diamagnetic contributions of the substrates.[312]

Conclusions

Hydrogen as a clean energy source is making significant inroads with government investments across the globe. Due to the unique properties of hydrogen, developing reliable sensors for its application in various parts of the supply chain is essential from safety, environmental, and economic perspectives. The search for a gas sensor fitting all the requirements of a specific application is a difficult task. There are many different hydrogen sensor technologies with different advantages and disadvantages. In order to make an informed decision, one has to understand the specifics of the different technologies and how they are compatible with the application. For example, a remotely operated sensor will preferably require low power consumption compared to a sensor at a regularly maintained facility. The background conditions such as humidity, pollutants, presence of VOCs, operating temperature, and pressure should all be taken into consideration while choosing a sensor for a specific application. Guidance in sensor selection can be obtained by answers to questions such as; (i) is it possible to put a sensor close to a possible leak site or is it necessary to test from a distance? (ii) how sensitive must the sensor be and what range of concentrations with what resolution is required? (iii) how selective must the sensor be? One has to keep in mind that there is no handbook for the perfect

Table VIII. Overview of several commercially available piezoelectric gas sensors showing their concentration ranges, power consumptions, cross sensitivities, and lifetime.

Gas	Manufacturer	Concentration range	Power consumption	Cross sensitivities	Lifetime	References
H_2	ATO	0–5000 ppm	3.7 W			301
	Industrial Scientific	0–500/1000/2000 ppm				302
	Analytical Technology Inc.	0–500/2000 ppm				303
NH_3	Industrial Scientific	0–500 ppm				304
	GasSensing	0–50/500 ppm				305
	BW Honeywell	0 to 100 ppm				305
CH_4	Macurco	0 to 50% LEL Sensor Range	0–240 V AC (50 to 60 Hz)	C_3H_8, CH_4, H_2		306

Table IX. Overview of acoustic and resistive based hydrogen gas sensors showing their concentration ranges, power consumptions, cross sensitivities, and lifetime.

Gas	Manufacturer	Concentration Range	Power Consumption	Cross sensitivities	Lifetime	Technology	References
H_2	H2Scan	0.4–5%	10–15 W	None listed		Diode/resistive	313
CH_4	Riken Keiki Co, Ltd	25–50 $MJ*m^{-3}$	5–18 W	Paraffinic hydrocarbons		Optical and acoustic	310
All	Det-Tronics	undefined	2–3.5 W	Not selective	3 years	acoustic	309
All	Emerson Rosemount™	undefined	6 W	Not selective	18 months	acoustic	314
All	Dräger Polytron® 6100 EC WL	undefined		Not selective	2 years		315

solution for any application. Most of the time, one will have to accept a compromise of selectivity, price, power consumption, size, lifetime, concentration range, or other sensor characteristic. At the same time this means that the market needs improved sensor solutions regarding price, performance (sensitivity and selectivity), power consumption and stability (ranges of temperatures, pressures, and humidity levels as well as lifetime). The research in the field of hydrogen sensors is ongoing and yielding promising new technology. We expect the current commercial sensors to play an important role in implementing the hydrogen economy while also recognizing the need to develop more robust, lower cost, intrinsically safe, sensitive, fast responding, stable, and selective hydrogen, methane and ammonia sensors. Combinations of new materials, operating protocols, and computational methods, many surveyed herein, will improve our ability to achieve effective and efficient rollout of the hydrogen energy solutions.

ORCID

Kannan Ramaiyan https://orcid.org/0000-0003-0204-7550
Lok-kun Tsui https://orcid.org/0000-0001-7381-0686
Joseph R. Stetter https://orcid.org/0000-0002-7839-0980
Tamara Russ https://orcid.org/0000-0001-6856-0088
Fernando Garzon https://orcid.org/0000-0002-4511-9932
Rangachary Mukundan https://orcid.org/0000-0002-5679-3930

References

1. J. O. Bockris and A. J. Appleby, "The hydrogen economy - an ultimate economy." *Env. This Mon.*, **1**, 29 (1972).
2. J. O. M. Bockris, "The hydrogen economy: its history." *Int. J. Hydrog. Energy*, **38**, 2579 (2013).
3. *DOE Establishes Bipartisan Infrastructure Law's $9.5 Billion Clean Hydrogen Initiatives*. Energy.gov. https://energy.gov/articles/doe-establishes-bipartisan-infrastructure-laws-95-billion-clean-hydrogen-initiatives (accessed 2023-05-08).
4. *HysetCo moves to run 600 hydrogen cabs in Paris*. electrive.com. https://electrive.com/2021/01/26/hysetco-moves-to-run-600-hydrogen-cabs-in-paris/ (accessed 2022-12-03) N. Manthey.
5. C. Palmer, "Hydrogen-powered trains start to roll." *Engineering*, **11**, 9 (2022).
6. IEA report, *Global Hydrogen REVIEW*, **2021**, https://iea.blob.core.windows.net/assets/5bd46d7b-906a-4429-abda-e9c507a62341/GlobalHydrogenReview2021.pdf (accessed 2022-10-21), 1 (2021).
7. J. Ogden, A. M. Jaffe, D. Scheitrum, Z. McDonald, and M. Miller, "Natural gas as a bridge to hydrogen transportation fuel: insights from the literature." *Energy Policy*, **115**, 317 (2018).
8. J. S. Cardoso, V. Silva, R. C. Rocha, M. J. Hall, M. Costa, and D. Eusébio, "Ammonia as an energy vector: current and future prospects for low-carbon fuel applications in internal combustion engines." *J. Clean. Prod.*, **296**, 126562 (2021).
9. D. R. MacFarlane, P. V. Cherepanov, J. Choi, B. H. R. Suryanto, R. Y. Hodgetts, J. M. Bakker, F. M. Ferrero Vallana, and A. N. Simonov, "A roadmap to the ammonia economy." *Joule*, **4**, 1186 (2020).
10. *Annual Report Mileage for Natural Gas Transmission & Gathering Systems | PHMSA*. https://phmsa.dot.gov/data-and-statistics/pipeline/annual-report-mileage-natural-gas-transmission-gathering-systems (accessed 2023-01-01).
11. B. Ott, L. Delafontaine, N. A. Welchert, S. Dee, and A. Reza, "Ensuring natural gas infrastructure is suitable for hydrogen service." *Process Saf. Prog.*, **42**, 213 (2023).
12. D. W. Kang and J. H. Holbrook, "Use of NH3 fuel to achieve deep greenhouse gas reductions from US transportation." *Energy Rep*, **1**, 164 (2015).
13. H. Ishaq and I. Dincer, "A comprehensive study on using new hydrogen-natural gas and ammonia-natural gas blends for better performance." *J. Nat. Gas Sci. Eng.*, **81**, 103362 (2020).
14. B. Mahant, P. Linga, and R. Kumar, "Hydrogen economy and role of hythane as a bridging solution: a perspective review." *Energy Fuels*, **35**, 15424 (2021).
15. IEA report, *The Future of Hydrogen* (2019), https://hydrogenexpo.com/media/9370/the_future_of_hydrogen_iea.pdf (accessed 2022-10-22)(International Energy Agency, Japan) 1.
16. S. Halley, L. Tsui, and F. Garzon, "Combined mixed potential electrochemical sensors and artificial neural networks for the quantificationand identification of methane in natural gas emissions monitoring." *J. Electrochem. Soc.*, **168**, 097506 (2021).
17. R. A. Alvarez et al., "Assessment of Methane emissions from the U.S. oil and gas supply chain." *Science*, **361**, 186 (2018).
18. R. W. Howarth and M. Z. Jacobson, "How green is blue hydrogen?" *Energy Sci. Eng.*, **9**, 1676 (2021).
19. J. S. Rutherford, E. D. Sherwin, A. P. Ravikumar, G. A. Heath, J. Englander, D. Cooley, D. Lyon, M. Omara, Q. Langfitt, and A. R. Brandt, "Closing the methane gap in US oil and natural gas production emissions inventories." *Nat. Commun.*, **12**, 4715 (2021).
20. T. Longden, F. J. Beck, F. Jotzo, R. Andrews, and M. Prasad, "Clean" hydrogen?—comparing the emissions and costs of fossil fuel versus renewable electricity based hydrogen." *Appl. Energy*, **306**, 118145 (2022).
21. R. Mansoor and M. Tahir, "Recent developments in natural gas flaring reduction and reformation to energy-efficient fuels: a review." *Energy Fuels*, **35**, 3675 (2021).
22. L. H. Denoyer, A. Benavidez, F. H. Garzon, and K. P. Ramaiyan, "Highly stable doped barium niobate based electrocatalysts for effective electrochemical coupling of methane to ethylene." *Adv. Mater. Interfaces*, **9**, 2200796 (2022).
23. D. Kwak, Y. Lei, and R. Maric, "Ammonia gas sensors: a comprehensive review." *Talanta*, **204**, 713 (2019).
24. S. Hardman and G. Tal, "Who are the early adopters of fuel cell vehicles?" *Int. J. Hydrog. Energy*, **43**, 17857 (2018).
25. S. Foorginezhad, M. Mohseni-Dargah, Z. Falahati, R. Abbassi, A. Razmjou, and M. Asadnia, "Sensing advancement towards safety assessment of hydrogen fuel cell vehicles." *J. Power Sources*, **489**, 229450 (2021).
26. C. San Marchi, E. S. Hecht, I. W. Ekoto, K. M. Groth, C. LaFleur, B. P. Somerday, R. Mukundan, T. Rockward, J. Keller, and C. W. James, "Overview of the DOE hydrogen safety, codes and standards program, part 3. Advances in research and development to enhance the scientific basis for hydrogen regulations, codes and standards." *Int. J. Hydrog. Energy*, **42**, 7263 (2017).
27. US Drive - Hydrogen Delivery Technical Team Roadmap July 2017. https://energy.gov/sites/prod/files/2017/08/f36/hdtt_roadmap_July2017.pdf 2017.
28. W. J. Buttner, M. B. Post, R. Burgess, and C. Rivkin, "An overview of hydrogen safety sensors and requirements." *Int. J. Hydrog. Energy*, **36**, 2462 (2011).
29. T. Sahoo and P. Kale, "Work function-based metal–oxide–semiconductor hydrogen sensor and its functionality: a review." *Adv. Mater. Interfaces*, **8**, 2100649 (2021).
30. Y. Luo, C. Zhang, B. Zheng, X. Geng, and M. Debliquy, "Hydrogen sensors based on noble metal doped metal-oxide semiconductor: a review." *Int. J. Hydrog. Energy*, **42**, 20386 (2017).
31. P. S. Chauhan and S. Bhattacharya, "Hydrogen gas sensing methods, materials, and approach to achieve parts per billion level detection: a review." *Int. J. Hydrog. Energy*, **44**, 26076 (2019).
32. Y. Nemirovsky, S. Stolyarova, T. Blank, S. Bar-Lev, A. Svetlitza, A. Zviagintsev, and I. Brouk, "A new pellistor-like gas sensor based on micromachined CMOS transistor." *IEEE Trans. Electron Devices*, **65**, 5494 (2018).
33. I. B. Ocko and S. P. Hamburg, "Climate consequences of hydrogen emissions." *Atmospheric Chem. Phys.*, **22**, 9349 (2022).
34. T. Hübert, L. Boon-Brett, G. Black, and U. Banach, "Hydrogen sensors—a review." *Sens. Actuators B Chem.*, **157**, 329 (2011).
35. G. Korotcenkov, S. D. Han, and J. R. Stetter, "Review of electrochemical hydrogen sensors." *Chem. Rev.*, **109**, 1402 (2009).
36. E. Gorbova, G. Balkourani, C. Molochas, D. Sidiropoulos, A. Brouzgou, A. Demin, and P. Tsiakaras, "Brief review on high-temperature electrochemical hydrogen sensors." *Catalysts*, **12**, 1647 (2022).
37. C. Wang, J. Yang, J. Li, C. Luo, X. Xu, and F. Qian, "Solid-state electrochemical hydrogen sensors: a review." *Int. J. Hydrog. Energy*, **48**, 31377 (2023).
38. H. Gu, Z. Wang, and Y. Hu, "Hydrogen gas sensors based on semiconductor oxide nanostructures." *Sensors*, **12**, 5517 (2012).
39. W.-T. Koo, H.-J. Cho, D.-H. Kim, Y. H. Kim, H. Shin, R. M. Penner, and I.-D. Kim, "Chemiresistive hydrogen sensors: fundamentals, recent advances, and challenges." *ACS Nano*, **14**, 14284 (2020).
40. I.-D. Kim, A. Rothschild, and H. L. Tuller, "Advances and new directions in gas-sensing devices." *Diam. Jubil. Issue*, **61**, 974 (2013).
41. J. Hu, Y. Sun, Y. Xue, M. Zhang, P. Li, K. Lian, S. Zhuiykov, W. Zhang, and Y. Chen, "Highly sensitive and ultra-fast gas sensor based on CeO2-Loaded In2O3 hollow spheres for Ppb-level hydrogen detection." *Sens. Actuators B Chem.*, **257**, 124 (2018).
42. J.-H. Lee, J.-H. Kim, J.-Y. Kim, A. Mirzaei, H. W. Kim, and S. S. Kim, "Ppb-Level selective hydrogen gas detection of Pd-functionalized In2O3-Loaded ZnO nanofiber gas sensors." *Sensors*, **19**, 4276 (2019).
43. J. Zhang, L. Liu, Y. Yang, Q. Huang, D. Li, and D. Zeng, "A review on two-dimensional materials for chemiresistive- and FET-type gas sensors." *Phys. Chem. Chem. Phys.*, **23**, 15420 (2021).
44. N. Joshi, T. Hayasaka, Y. Liu, H. Liu, O. N. Oliveira, and L. Lin, "A review on chemiresistive room temperature gas sensors based on metal oxide nanostructures, graphene and 2D transition metal dichalcogenides." *Microchim. Acta*, **185**, 213 (2018).
45. S. Gasso, M. K. Sohal, and A. Mahajan, "MXene modulated SnO2 gas sensor for ultra-responsive room-temperature detection of NO2." *Sens. Actuators B Chem.*, **357**, 131427 (2022).
46. S. Gasso and A. Mahajan, "MXene decorated tungsten trioxide nanocomposite-based sensor capable of detecting NO2 gas down to Ppb-Level at room temperature." *Mater. Sci. Semicond. Process.*, **152**, 107048 (2022).
47. E. Lee, A. VahidMohammadi, Y. S. Yoon, M. Beidaghi, and D.-J. Kim, "Two-dimensional vanadium carbide MXene for gas sensors with ultrahigh sensitivity toward nonpolar gases." *ACS Sens.*, **4**, 1603 (2019).
48. J.-Y. Jeon, S.-J. Park, and T.-J. Ha, "Functionalization of zinc oxide nanoflowers with palladium nanoparticles via microwave absorption for room temperature-operating hydrogen gas sensors in the Ppb level." *ACS Appl. Mater. Interfaces*, **13**, 25082 (2021).
49. I. Darmadi, F. A. A. Nugroho, and C. Langhammer, "High-performance nanostructured palladium-based hydrogen sensors—current limitations and strategies for their mitigation." *ACS Sens.*, **5**, 3306 (2020).

50. G. Behzadi Pour, L. Fekri Aval, M. Nasiri Sarvi, S. Fekri Aval, and H. Nazarpour Fard, "Hydrogen sensors: palladium-based electrode." *J. Mater. Sci., Mater. Electron.*, **30**, 8145 (2019).
51. K. Katahira, H. Matsumoto, H. Iwahara, K. Koide, and T. Iwamoto, "A solid electrolyte hydrogen sensor with an electrochemically-supplied hydrogen standard." *Sens. Actuators B Chem.*, **73**, 130 (2001).
52. E. Miliutina, O. Guselnikova, S. Chufistova, Z. Kolska, R. Elashnikov, V. Burtsev, P. Postnikov, V. Svorcik, and O. Lyutakov, "Fast and all-optical hydrogen sensor based on gold-coated optical fiber functionalized with metal–organic framework layer." *ACS Sens.*, **4**, 3133 (2019).
53. D. Berndt, J. Muggli, F. Wittwer, C. Langer, S. Heinrich, T. Knittel, and R. Schreiner, "MEMS-Based thermal conductivity sensor for hydrogen gas detection in automotive applications." *Sens. Actuators Phys.*, **305**, 111670 (2020).
54. N. Miura, T. Sato, S. A. Anggraini, H. Ikeda, and S. Zhuiykov, "A review of mixed-potential type zirconia-based gas sensors." *Ionics*, **20**, 901 (2014).
55. K. P. Ramaiyan and R. Mukundan, "Editors' choice—review—recent advances in mixed potential sensors." *J. Electrochem. Soc.*, **167**, 037547 (2020).
56. S. Halley, K. P. Ramaiyan, L. Tsui, and F. Garzon, "A review of zirconia oxygen, NOx, and mixed potential gas sensors—history and current trends." *Sens. Actuators B Chem.*, **370**, 132363 (2022).
57. R. Mukundan, E. L. Brosha, and F. H. Garzon, "Mixed potential hydrocarbon sensors based on a YSZ electrolyte and oxide electrodes." *J. Electrochem. Soc.*, **150**, H279 (2003).
58. F. H. Garzon, R. Mukundan, and E. L. Brosha, "Solid-state mixed potential gas sensors: theory, experiments and challenges." *Solid State Ion.*, **136–137**, 633 (2000).
59. Y. Chao, S. Yao, W. J. Buttner, and J. R. Stetter, "Amperometric Sensor for Selective and Stable Hydrogen Measurement." *Sens. Actuators B Chem.*, **106**, 784 (2005).
60. K. Arora, S. Srivastava, P. R. Solanki, and N. K. Puri, "Electrochemical hydrogen gas sensing employing palladium oxide/reduced graphene oxide (PdO-RGO) nanocomposites." *IEEE Sens. J.*, **19**, 8262 (2019).
61. W. Li, L. Huang, H. Sun, B. Wang, Q. Lu, X. Liang, F. Liu, F. Liu, P. Sun, and G. Lu, "Room temperature hydrogen sensor based on nafion and Pd/CF sensing electrode." *Sens. Actuators B Chem.*, **366**, 132014 (2022).
62. E. Jayanthi, N. Murugesan, S. Anthonysamy, and C. Ramesh, "Comparative study of sensing behavior of brush coated, electrodeposited and pulsed electrodeposited Pt/GDE based amperometric hydrogen sensors." *Sens. Actuators B Chem.*, **273**, 488 (2018).
63. S.-W. Jung, E. K. Lee, J. H. Kim, and S.-Y. Lee, "High-concentration nafion-based hydrogen sensor for fuel-cell electric vehicles." *Solid State Ion.*, **344**, 115134 (2020).
64. J.-S. Do, Y.-Y. Chen, and M.-L. Tsai, "Planar solid-state amperometric hydrogen gas sensor based on Nafion®/Pt/nano-structured polyaniline/Au/Al2O3 electrode." *Int. J. Hydrog. Energy*, **43**, 14848 (2018).
65. J. M. Ohi, N. Vanderborgh, G. Voecks, S. Ahmed, Kumar, D. Papadius, and T. Rockward (ed.), Hydrogen Fuel Quality Specifications for Polymer Electrolyte Fuel Cells in Road Vehicles. (2017) *https://energy.gov/sites/prod/files/2017/01/f34/fcto_h2_fuel_quality_specs_pem_fc_road_vehicles.pdf*.
66. X. Cheng, Z. Shi, N. Glass, L. Zhang, J. Zhang, D. Song, Z.-S. Liu, H. Wang, and J. Shen, "A review of PEM hydrogen fuel cell contamination: impacts, mechanisms, and mitigation." *J. Power Sources*, **165**, 739 (2007).
67. M. Angelo, K. Bethune, and R. Rocheleau, "The impact of sub Ppm carbon monoxide and Ppm level CO/Toluene and Methylcyclohexane/CO mixtures on PEMFC performance and durability." *ECS Trans.*, **28**, 169 (2010).
68. F. Garzon, F. A. Uribe, T. Rockward, I. G. Urdampilleta, and E. L. Brosha, "The impact of hydrogen fuel contaminates on long-term PMFC performance." *ECS Trans.*, **3**, 695 (2006).
69. D. Imamura, D. Ebata, Y. Hshimasa, M. Akai, and S. Watanabe, "Impact of hydrogen fuel impurities on PEMFC performance." *SAE Trans.*, **116**, 621 (2007).
70. F. Garzon, T. Lopes, T. Rockward, J.-M. Sansiñena, B. Kienitz, and R. Mukundan, "The impact of impurities on long-term PEMFC performance." *ECS Trans.*, **25**, 1575 (2009).
71. K. Narusawa, M. Hayashida, Y. Kamiya, H. Roppongi, D. Kurashima, and K. Wakabayashi, "Deterioration in fuel cell performance resulting from hydrogen fuel containing impurities: poisoning effects by CO, CH4, HCHO and HCOOH." *JSAE Rev.*, **24**, 41 (2003).
72. X. Zhang, H. M. Galindo, H. F. Garces, P. Baker, X. Wang, U. Pasaogullari, S. L. Suib, and T. Molter, "Influence of formic acid impurity on proton exchange membrane fuel cell performance." *J. Electrochem. Soc.*, **157**, B409 (2010).
73. W. Shi, B. Yi, M. Hou, and Z. Shao, "The effect of H2S and CO mixtures on PEMFC performance." *Int. J. Hydrog. Energy*, **32**, 4412 (2007).
74. J. St-Pierre, M. Angelo, K. Bethune, J. Ge, S. Higgins, T. V. Reshetenko, M. B. V. Virji, and Y. Zhai, "PEMFC contamination - fundamentals and outlook." *ECS Trans.*, **61**, 1 (2014).
75. K. Arrhenius, T. Bacquart, K. Schröter, M. Carré, B. Gozlan, C. Beurey, and C. Blondeel, "Detection of contaminants in hydrogen fuel for fuel cell electrical vehicles with sensors—available technology, testing protocols and implementation challenges." *Processes*, **10**, 20 (2022).
76. E. L. Brosha, T. Rockward, C. J. Romero, M. S. Wilson, C. R. Kreller, and R. Mukundan, Hydrogen Fuel Quality Analyzer with Self-Humidifying Electrochemical Cell and Methods of Testing Fuel Quality. US10490833B1, November 26, 2019. https://patents.google.com/patent/US10490833B1/en?inventor=Brosha&oq=Brosha+&page=1 (accessed 2022-12-08).
77. R. Mukundan, E. L. Brosha, C. J. Romero, D. Poppe, and T. Rockward, "Development of an electrochemical hydrogen contaminant detector." *J. Electrochem. Soc.*, **167**, 147507 (2020).
78. Z. Noda, K. Hirata, A. Hayashi, S. Taniguchi, N. Nakazato, A. Seo, I. Yasuda, S. Ariura, H. Shinkai, and K. Sasaki, "PEFC-type impurity sensors for hydrogen fuels." *Int. J. Hydrog. Energy*, **37**, 16256 (2012).
79. Z. Noda et al., "Hydrogen pump-type impurity sensors for hydrogen fuels." *Int. J. Hydrog. Energy*, **42**, 3281 (2017).
80. R. Borup et al., "Scientific aspects of polymer electrolyte fuel cell durability and degradation." *Chem. Rev.*, **107**, 3904 (2007).
81. K. Hu and D. Yang, "Studies on the effects of NH3 in H2 and air on the performance of PEMFC." *Energies*, **14**, 6556 (2021).
82. M. M. Tripathi, K. E. Eseller, F.-Y. Yueh, and J. P. Singh, "An optical sensor for multi-species impurity monitoring in hydrogen fuel." *Sens. Actuators B Chem.*, **171-172**, 416 (2012).
83. S. W. Kim, B. A. Trisna, M. Yin, J. Lim, T. K. Ahn, and J. Lee, "Development of a hydrogen impurity analyzer based on mobile-gas chromatography for online hydrogen fuel monitoring." *Int. J. Hydrog. Energy*, **48**, 13012 (2023).
84. M. W. Melaina, O. Antonia, and M. Penev, "Blending hydrogen into natural gas pipeline networks: a review of key issues." *Technical Report*, **NREL/TP-5600-51995**, 0 (2013).
85. *HYTHANE Trademark of ENGIE. Application Number: 000379164 :: Trademark Elite Trademarks*. https://trademarkelite.com (accessed 2023-09-08) T. Elite.
86. *Innovations | Eden Innovations*. https://edeninnovations.com/innovations/ (accessed 2023-09-20).
87. ☑G. Di Lullo, T. Giwa, A. Okunlola, M. Davis, T. Mehedi, A. O. Oni, and A. Kumar, "Large-scale long-distance land-based hydrogen transportation systems: a comparative techno-economic and greenhouse gas emission assessment." *Int. J. Hydrog. Energy*, **47**, 35293 (2022).
88. T. Strahl, J. Herbst, A. Lambrecht, E. Maier, J. Steinebrunner, and J. Wöllenstein, "Methane leak detection by tunable laser spectroscopy and mid-infrared imaging." *Appl. Opt.*, **60**, C68 (2021).
89. E E Karpov, E F. Karpov, A Suchkov, S. Mironov, A. Baranov, V. Sleptsov, and L. Calliari, "Energy efficient planar catalytic sensor for methane measurement." *Sens. Actuators Phys.*, **194**, 176 (2013).
90. R. Wu, L. Tian, H. Li, H. Liu, J. Luo, X. Tian, Z. Hua, Y. Wu, and S. Fan, "A selective methane gas sensor based on metal oxide semiconductor equipped with an on-chip microfilter." *Sens. Actuators B Chem.*, **359**, 131557 (2022).
91. R. K. Jha, "Non-dispersive infrared gas sensing technology: a review." *IEEE Sens. J.*, **22**, 6 (2022).
92. S. Fanchenko, A. Baranov, A. Savkin, and V. Sleptsov, "LED-based NDIR natural gas analyzer." *IOP Conf. Ser.: Mater. Sci. Eng.*, **108**, 012036 (2016).
93. N. P. Ayerden, G. Graaf, P. de; Enoksson, and R. F. Wolffenbuttel, "A highly miniaturized NDIR methane sensor." *Proc. SPIE 9888, Micro-Optics 2016*, **98880D**, 57 (2016).
94. E. R. Crosson, "A cavity ring-down analyzer for measuring atmospheric levels of methane, carbon dioxide, and water vapor." *Appl. Phys. B*, **92**, 403 (2008).
95. M. D. Wheeler, S. M. Newman, A. J. Orr-Ewing, and M. N. R. Ashfold, "Cavity ring-down spectroscopy." *J. Chem. Soc. Faraday Trans.*, **94**, 337 (1998).
96. L. E. Mchale, B. Martinez, T. W. Miller, and A. P. Yalin, "Open-path cavity ring-down methane sensor for mobile monitoring of natural gas emissions." *Opt. Express*, **27**, 20084 (2019).
97. J. Shemshad, S. M. Aminossadati, and M. S. Kizil, "A review of developments in near infrared methane detection based on tunable diode laser." *Sens. Actuators B Chem.*, **171–172**, 77 (2012).
98. J. Manne, T. Q. Bui, and C. R. Webster, "Determination of foreign broadening coefficients for methane lines targeted by the tunable laser spectrometer (TLS) on the mars curiosity rover." *J. Quant. Spectrosc. Radiat. Transf.*, **191**, 59 (2017).
99. T. Iseki, H. Tai, and K. Kimura, "A portable remote methane sensor using a tunable diode laser." *Meas. Sci. Technol.*, **11**, 594 (2000).
100. S. Dello Russo, S. Zhou, A. Zifarelli, P. Patimisco, A. Sampaolo, M. Giglio, D. Iannuzzi, and V. Spagnolo, "Photoacoustic spectroscopy for gas sensing: a comparison between piezoelectric and interferometric readout in custom quartz tuning forks." *Photoacoustics*, **17**, 100155 (2020).
101. M. Triki, T. Nguyen Ba, and A. Vicet, "Compact sensor for methane detection in the mid infrared region based on quartz enhanced photoacoustic spectroscopy." *Infrared Phys. Technol.*, **69**, 74 (2015).
102. E. Tuboly, A. Szabó, G. Erős, Á. Mohácsi, G. Szabó, R. Tengölics, G. Rákhely, and M. Boros, "Determination of endogenous methane formation by photoacoustic spectroscopy." *J. Breath Res.*, **7**, 046004 (2013).
103. V. Zéninari, B. Parvitte, D. Courtois, V. A. Kapitanov, and Y. N. Ponomarev, "Methane detection on the sub-ppm level with a near-infrared diode laser photoacoustic sensor." *Infrared Phys. Technol.*, **44**, 253 (2003).
104. O. Hennig, R. Strzoda, E. Mágori, E. Chemisky, C. Tump, M. Fleischer, H. Meixner, and I. Eisele, "Hand-Held unit for simultaneous detection of methane and ethane based on NIR-absorption spectroscopy." *Sens. Actuators B Chem.*, **95**, 151 (2003).
105. A. Sampaolo, S. Csutak, P. Patimisco, M. Giglio, G. Menduni, V. Passaro, F. K. Tittel, M. Deffenbaugh, and V. Spagnolo, "Methane, ethane and propane detection using a compact quartz enhanced photoacoustic sensor and a single interband cascade laser." *Sens. Actuators B Chem.*, **282**, 952 (2019).
106. P. Luo, J. Harrist, G. Menduni, R. Mesdour, N. StMichel, and A. Sampaolo, "Simultaneous detection of methane, ethane, and propane by QEPAS sensors for on-site hydrocarbon characterization and production monitoring." *ACS Omega*, **7**, 3395 (2022).

107. *CMR Group launches new natural gas sensor*. Hydrocarbon Engineering. https://hydrocarbonengineering.com/product-news/19062019/cmr-group-launches-new-natural-gas-sensor/ (accessed 2023-09-20).
108. A. Maity, M. Pal, G. D. Banik, S. Maithani, and M. Pradhan, "Cavity ring-down spectroscopy using an EC-QCL operating at 7.5 Mm for direct monitoring of methane isotopes in air." *Laser Phys. Lett.*, **14**, 115701 (2017).
109. J. W. Pohlman, M. Casso, C. Magen, and E. Bergeron, "Discrete sample introduction module for quantitative and isotopic analysis of methane and other gases by cavity ring-down spectroscopy." *Environ. Sci. Technol.*, **55**, 12066 (2021).
110. B. Martinez, T. W. Miller, and A. P. Yalin, "Cavity ring-down methane sensor for small unmanned aerial systems." *Sensors*, **20**, 454 (2020).
111. N. J. Pekney, J. R. Diehl, D. Ruehl, J. Sams, G. Veloski, A. Patel, C. Schmidt, and T. Card, "Measurement of methane emissions from abandoned oil and gas wells in hillman state park, pennsylvania." *Carbon Manag.*, **9**, 165 (2018).
112. S. Yang, R. W. Talbot, M. B. Frish, L. M. Golston, N. F. Aubut, M. A. Zondlo, C. Gretencord, and J. McSpiritt, "Natural gas fugitive leak detection using an unmanned aerial vehicle: measurement system description and mass balance approach." *Atmosphere*, **9**, 383 (2018).
113. T. Aldhafeeri, M.-K. Tran, R. Vrolyk, M. Pope, and M. Fowler, "A review of methane gas detection sensors: recent developments and future perspectives." *Inventions*, **5**, 28 (2020).
114. P. Shuk, C. McGuire, and E. Brosha, "Methane gas sensing technologies in combustion: comprehensive review." *Sens. Transducers*, **229** (2019).
115. X.-T. Yin et al., "Tin dioxide nanoparticles with high sensitivity and selectivity for gas sensors at Sub-Ppm level of hydrogen gas detection." *J. Mater. Sci., Mater. Electron.*, **30**, 14687 (2019).
116. N.-H. Park, T. Akamatsu, T. Itoh, N. Izu, and W. Shin, "Calorimetric thermo-electric gas sensor for the detection of hydrogen, methane and mixed gases." *Sensors*, **14**, 8350 (2014).
117. S. Basu and P. K. Basu, "Nanocrystalline metal oxides for methane sensors: role of noble metals." *J. Sens.*, **2009**, 861968 (2009).
118. A. Dey, "Semiconductor metal oxide gas sensors: a review." *Mater. Sci. Eng. B*, **229**, 206 (2018).
119. T. Hong, J. T. Culp, K.-J. Kim, J. Devkota, C. Sun, and P. R. Ohodnicki, "State-of-the-art of methane sensing materials: a review and perspectives." *TrAC, Trends Anal. Chem.*, **125**, 115820 (2020).
120. P. K. Basu, S. K. Jana, H. Saha, and S. Basu, "Low temperature methane sensing by electrochemically grown and surface modified ZnO thin films." *Sens. Actuators B Chem.*, **135**, 81 (2008).
121. G. Fedorenko, L. Oleksenko, N. Maksymovych, G. Skolyar, and O. Ripko, "Semiconductor gas sensors based on Pd/SnO2 nanomaterials for methane detection in air." *Nanoscale Res. Lett.*, **12**, 329 (2017).
122. G. V. Fedorenko, L. P. Oleksenko, N. P. Maksymovych, and I. P. Matushko, "Semiconductor adsorption sensors based on nanosized Pt/SnO2 materials and their sensitivity to methane." *Russ. J. Phys. Chem. A*, **89**, 2259 (2015).
123. L. P. Oleksenko, G. V. Fedorenko, and N. P. Maksymovych, "Platinum-containing adsorption-semiconductor sensors based on nanosized tin dioxide for methane detection." *Theor. Exp. Chem.*, **53**, 259 (2017).
124. G. Tournier and C. Pijolat, "Selective filter for SnO2-based gas sensor: application to hydrogen trace detection." *Sens. Actuators B Chem.*, **106**, 553 (2005).
125. N. Lu, S. Fan, Y. Zhao, B. Yang, Z. Hua, and Y. Wu, "A selective methane gas sensor with printed catalytic films as active filters." *Sens. Actuators B Chem.*, **347**, 130603 (2021).
126. Y. Zhao, S. Wang, W. Yuan, S. Fan, Z. Hua, Y. Wu, and X. Tian, "Selective detection of methane by Pd-In2O3 sensors with a catalyst filter film." *Sens. Actuators B Chem.*, **328**, 129030 (2021).
127. Y. Cho, K. M. Smits, S. N. Riddick, and D. J. Zimmerle, "Calibration and field deployment of low-cost sensor network to monitor underground pipeline leakage." *Sens. Actuators B Chem.*, **355**, 131276 (2022).
128. P. K. Sekhar, J. Kysar, E. L. Brosha, and C. R. Kreller, "Development and testing of an electrochemical methane sensor." *Sens. Actuators B Chem.*, **228**, 162 (2016).
129. B. Yang, J. Xu, C. Wang, and J. Xiao, "A potentiometric sensor based on SmMn2O5 sensing electrode for methane detection." *Mater. Chem. Phys.*, **245**, 122679 (2020).
130. I. Irakulis-Loitxate, "Satellite-based survey of extreme methane emissions in the permian basin." *Sci. Adv.*, **7**, eabf4507 (2021).
131. B. A. Ulrich, M. Mitton, E. Lachenmeyer, A. Hecobian, D. Zimmerle, and K. M. Smits, "Natural gas emissions from underground pipelines and implications for leak detection." *Environ. Sci. Technol. Lett.*, **6**, 401 (2019).
132. S. Tian, K. M. Smits, Y. Cho, S. N. Riddick, D. J. Zimmerle, and A. Duggan, "Estimating methane emissions from underground natural gas pipelines using an atmospheric dispersion-based method." *Elem. Sci. Anthr.*, **10**, 00045 (2022).
133. J. B. A. Gomes, J. J. P. C. Rodrigues, R. A. L. Rabêlo, N. Kumar, and S. Kozlov, "IoT-Enabled gas sensors: technologies, applications, and opportunities." *J. Sens. Actuator Netw.*, **8**, 57 (2019).
134. *UL 2034, Single and Multiple Station Carbon Monoxide Alarms*. https://shopulstandards.com/ProductDetail.aspx?productId=UL2034 (accessed 2023-04-27).
135. G. J. May, A. Davidson, and B. Monahov, "Lead batteries for utility energy storage: a review." *J. Energy Storage*, **15**, 145 (2018).
136. J. H. Rowland, L. Yuan, R. A. Thomas, and L. Zhou, "Evaluation of different carbon monoxide sensors for battery charging stations." *Min. Metall. Explor.*, **36**, 245 (2019).
137. M. Ródenas García et al., "Review of low-cost sensors for indoor air quality: features and applications." *Appl. Spectrosc. Rev.*, **57**, 747 (2022).
138. L. Spinelle, M. Gerboles, G. Kok, S. Persijn, and T. Sauerwald, "Review of portable and low-cost sensors for the ambient air monitoring of benzene and other volatile organic compounds." *Sensors*, **17**, 1520 (2017).
139. P. Raju and Q. Li, "Review—semiconductor materials and devices for gas sensors." *J. Electrochem. Soc.*, **169**, 057518 (2022).
140. I. C. Weber and A. T. Güntner, "Catalytic filters for metal oxide gas sensors." *Sens. Actuators B Chem.*, **356**, 131346 (2022).
141. J. van den Broek, I. C. Weber, A. T. Güntner, and S. E. Pratsinis, "Highly selective gas sensing enabled by filters." *Mater. Horiz.*, **8**, 661 (2021).
142. M. Hübner, A. Yuece, G. C. Mondragón Rodríguez, B. Saruhan, N. Barsan, and U. Weimar, "BaTi0,95Rh0,05O3 catalytic filter layer - a promising candidate for the selective Detection of CO in the presence of H2." *Eurosensor XXIV Conf.*, **5**, 107 (2010).
143. S. Xue, S. Cao, Z. Huang, D. Yang, and G. Zhang, "Improving gas-sensing performance based on MOS nanomaterials: a review." *Materials*, **14**, 4263 (2021).
144. M. Majder-Łopatka, T. Węsierski, A. Dmochowska, Z. Salamonowicz, and A. Polańczyk, "The influence of hydrogen on the indications of the electrochemical carbon monoxide sensors." *Sustainability*, **12**, 14 (2020).
145. Z. Yunusa, M. N. Hamidon, A Kaiser, and Z. Awang, "Gas sensors: a review." *Sens. Transducers*, **168**, 61 (2014).
146. A. T. Hodgson, "A review and a limited comparison of methods for measuring total volatile organic compounds in indoor air." *Indoor Air*, **5**, 247 (1995).
147. M. Fehér and P. A. Martin, "Tunable diode laser monitoring of atmospheric trace gas constituents." *Spectrochim. Acta. A. Mol. Biomol. Spectrosc.*, **51**, 1579 (1995).
148. T. Seesaard, N. Goel, M. Kumar, and C. Wongchoosuk, "Advances in gas sensors and electronic nose technologies for agricultural cycle applications." *Comput. Electron. Agric.*, **193**, 106673 (2022).
149. A. D. Wilson and M. Baietto, "Applications and advances in electronic-nose technologies." *Sensors*, **9**, 5099 (2009).
150. L. Cheng, Q.-H. Meng, A. J. Lilienthal, and P.-F. Qi, "Development of compact electronic noses: a review." *Meas. Sci. Technol.*, **32**, 062002 (2021).
151. P.-C. Chen, G. Shen, and C. Zhou, "Chemical sensors and electronic noses based on 1-D metal oxide nanostructures." *IEEE Trans. Nanotechnol.*, **7**, 668 (2008).
152. V. N. Mishra and R. P. Agarwal, "Sensitivity, response and recovery time of SnO2 based thick-film sensor array for H2, CO, CH4 and LPG." *Microelectron. J.*, **29**, 861 (1998).
153. K. Domanský, D. L. Baldwin, J. W. Grate, T. B. Hall, J. Li, M. Josowicz, and J. Janata, "Development and calibration of field-effect transistor-based sensor array for measurement of hydrogen and ammonia gas mixtures in humid air." *Anal. Chem.*, **70**, 473 (1998).
154. V. V. Sysoev, B. K. Button, K. Wepsiec, S. Dmitriev, and A. Kolmakov, "Toward the nanoscopic 'electronic nose': hydrogen vs carbon monoxide discrimination with an array of individual metal oxide nano- and mesowire sensors." *Nano Lett.*, **6**, 1584 (2006).
155. G. W. Hunter, J. Xu, P. G. Neudeck, D. B. Makel, B. Ward, and C. C. Liu, *Intelligent Chemical Sensor Systems for In-Space Safety Applications 42nd AIAA; ASME/SAE/ASEE Joint Propulsion Conf. & Exhibit (Sacramento, CA, 10–12 July 2006), 2006*.
156. *Development of Real-Time Particulate and Toxic-Gas Sensors for Firefighter Health and Safety*; Final report; 2019; p 71. https://engineering.case.edu/sites/default/files/Final%20report-Sensors-FY2014.pdf (accessed 2023-05-08) F. Takahashi.
157. G. W. Hunter, J. Williams, D. B. Makel, R. G. Johnson, A. M. Biaggi-Liabiosa, and C.-C. Liu, "Gas composition monitoring in cryogenic fluid transfer lines." *The Electrochemical Society, Inc.*, **MA2015-01**, 2167 (2015).
158. H. Sundgren, F. Winquist, and I. Lundstrom, "Artificial neural networks and statistical pattern recognition improve MOSFET gas sensor array calibration." *In TRANSDUCERS '91: 1991 International Conference on Solid-State Sensors and Actuators. Digest of Technical Papers; 1991; p. 574*.
159. H. Sundgren, F. Winquist, I. Lukkari, and I. Lundstrom, "Artificial neural networks and gas sensor arrays: quantification of individual components in a gas mixture." *Meas. Sci. Technol.*, **2**, 464 (1991).
160. J. Tsitron, C. R. Kreller, P. K. Sekhar, R. Mukundan, F. H. Garzon, E. L. Brosha, and A. V. Morozov, "Bayesian decoding of the ammonia response of a zirconia-based mixed-potential sensor in the presence of hydrocarbon interference." *Sens. Actuators B Chem.*, **192**, 283 (2014).
161. U. Javed, K. P. Ramaiyan, C. R. Kreller, E. L. Brosha, R. Mukundan, A. M. Sengupta, and A. V. Morozov, "Quantification of gas concentrations in NO/NO2/C3H8/NH3 mixtures using machine learning." *Sens. Actuators B Chem.*, **359**, 131589 (2022).
162. K. P. Ramaiyan, C. R. Kreller, E. L. Brosha, R. Mukundan, U. Javed, and A. V. Morozov, "Quantitative decoding of complex gas mixtures using mixed-potential sensor arrays." *ECS Trans.*, **75**, 107 (2016).
163. W. Zhang, L. Wang, J. Chen, X. Bi, C. Chen, J. Zhang, and V. Hans, "A novel gas recognition and concentration estimation model for an artificial olfactory system with a gas sensor array." *IEEE Sens. J.*, **21**, 18459 (2021).
164. P. Gwiżdż, A. Brudnik, and K. Zakrzewska, "Hydrogen detection with a gas sensor array—processing and recognition of dynamic responses using neural networks." *Metrol. Meas. Syst.*, **22**, 3 (2015).
165. Y. Sun, H. Zhang, T. Zhao, Z. Zou, B. Shen, and L. Yang, "A new convolutional neural network with random forest method for hydrogen sensor fault diagnosis." *IEEE Access*, **8**, 85421 (2020).
166. J. Li, B. Roche, J. M. Bull, P. R. White, T. G. Leighton, G. Provenzano, M. Dewar, and T. J. Henstock, "Broadband acoustic inversion for gas flux quantification—application to a methane plume at scanner pockmark, central north sea." *J. Geophys. Res. Oceans*, **125**, e2020JC016360 (2020).

167. D. Hollenbeck, D. Zulevic, and Y. Chen, "Advanced leak detection and quantification of methane emissions using SUAS." *Drones*, **5**, 117 (2021).
168. A. Shah, J. R. Pitt, H. Ricketts, J. B. Leen, P. I. Williams, K. Kabbabe, M. W. Gallagher, and G. Allen, "Testing the near-field gaussian plume inversion flux quantification technique using unmanned aerial vehicle sampling." *Atmospheric Meas. Tech.*, **13**, 1467 (2020).
169. J. Burgués, V. Hernández, A. J. Lilienthal, and S. Marco, "Gas distribution mapping and source localization using a 3D grid of metal oxide semiconductor sensors." *Sens. Actuators B Chem.*, **304**, 127309 (2020).
170. C. Bilgera, A. Yamamoto, M. Sawano, H. Matsukura, and H. Ishida, "Application of convolutional long short-term memory neural networks to signals collected from a sensor network for autonomous gas source localization in outdoor environments." *Sensors*, **18**, 4484 (2018).
171. B. Travis, M. Dubey, and J. Sauer, "Neural networks to locate and quantify fugitive natural gas leaks for a MIR detection system." *Atmospheric Environ. X*, **8**, 100092 (2020).
172. Y. M. Kwon, B. Oh, R. Purbia, H. Y. Chae, G. H. Han, S.-W. Kim, K.-J. Choi, Y. Lee, J. J. Kim, and J. M. Baik, "High-performance and self-calibrating multi-gas sensor interface to trace multiple gas species with sub-ppm level." *Sens. Actuators B Chem.*, **375**, 132939 (2023).
173. J. KIM, Y. W. Cho, and D. KIM, "Anomaly detection of environmental sensor data using recurrent neural network at the edge device." *In 2020 International Conference on Information and Communication Technology Convergence (ICTC); 2020; p. 1624*.
174. P. Beckman, R. Sankaran, C. Catlett, N. Ferrier, R. Jacob, and M. Papka, "Waggle: an open sensor platform for edge computing." *IEEE SENSORS*, **2016**, 1 (2016).
175. M. Satyanarayanan, "The emergence of edge computing." *Computer*, **50**, 30 (2017).
176. C. P. Filho, E. Marques, V. Chang, L. dos Santos, F. Bernardini, P. F. Pires, L. Ochi, and F. C. Delicato, "A systematic literature review on distributed machine learning in edge computing." *Sensors*, **22**, 2665 (2022).
177. B. Mondal, M. S. Meetei, J. Das, C. Roy Chaudhuri, and H. Saha, "Quantitative recognition of flammable and toxic gases with artificial neural network using metal oxide gas sensors in embedded platform." *Eng. Sci. Technol. Int. J.*, **18**, 229 (2015).
178. R. S. Filho, C.-L. Huang, B. Yu, R. Venkataramana, A. El-Messidi, D. Sharber, J. Westerheide, and N. Alkadi, "Semi-autonomous industrial robotic inspection: remote methane detection in oilfield." *In 2018 IEEE International Conference on Edge Computing (EDGE); 2018; p. 17*.
179. T. Kersnovski, F. Gonzalez, and K. Morton, "A UAV System for Autonomous Target Detection and Gas Sensing." *In 2017 IEEE Aerospace Conference; 2017; p. 1.*.
180. A. Simo, S. Dzitac, I. Dzitac, M. Frigura-Iliasa, and F. M. Frigura-Iliasa, "Air quality assessment system based on self-driven drone and LoRaWAN network." *Comput. Commun.*, **175**, 13 (2021).
181. F. M. Troeltsch, M. Engelmann, A. E. Scholz, F. Peter, J. Kaiser, and M. Hornung, "Hydrogen powered long haul aircraft with minimized climate impact." *Aerospace Research Central*, **0**, 2660 (2020).
182. R. V. V. Petrescu, A. Machin, K. Fontanez, J. C. Arango, F. M. Marquez, and F. I. T. Petrescu, "Hydrogen for aircraft power and propulsion." *Int. J. Hydrog. Energy*, **45**, 20740 (2020).
183. P. Tamburrano, L. Romagnuolo, E. Frosina, G. Caramia, E. Distaso, F. Sciatti, A. Senatore, P. De Palma, and R. Amirante, "Fuels systems and components for future airliners fuelled with liquid hydrogen." *IOP Publishing*, **2385**, 012041 (2022).
184. M. C. Massaro, R. Biga, A. Kolisnichenko, P. Marocco, A. H. A. Monteverde, and M. Santarelli, "Potential and technical challenges of on-board hydrogen storage technologies coupled with fuel cell systems for aircraft electrification." *J. Power Sources*, **555**, 232397 (2023).
185. G. W. Hunter, J. C. Xu, L. Evans, A. Biaggi-Labiosa, B. J. Ward, S. Rowe, D. B. Makel, C. C. Liu, P. Dutta, and G. M. Berger, "The development of micro/nano chemical sensor systems for aerospace applications." *SPIE*, **7679**, 215 (2010).
186. G. W. Hunter, D. L. Simon, J. C. Xu, A. Biaggi-Labiosa, S. Carranza, and D. Makel, "Aircraft ground demonstration of engine emissions monitoring system based on a gas microsensor array." *American Institute of Aeronautics and Astronautics*, **2014-3925** (2014).
187. G. W. Hunter, J. C. Xu, and D. Lukco, Miniaturized Metal (Metal Alloy)/ PdOx/ SiC Hydrogen and Hydrocarbon Gas Sensors US Patent US7389675B1. US7389675B1, June 24, 2008. https://patents.google.com/patent/US7389675/en (accessed 2023-09-22).
188. L.-Y. Chen, G. W. Hunter, P. G. Neudeck, D. Knight, C. C. Liu, and Q. H. Wu, "SiC-based gas sensors." *Proceedings of the Third International Symposium on Ceramic Sensors* (The Electrochemical Society, Inc, Pennington, NJ) 92 (1996).
189. G. Hunter, J. Xu, L. Dungan, B. Ward, S. Rowe, J. Williams, D. B. Makel, C.-C. Liu, and C. Chang, "Smart sensor systems for aerospace applications: from sensor development to application testing." *ECS Trans.*, **16**, 333 (2008).
190. G. Hunter, J. Xu, A. Biaggi-Labiosa, B. Ward, P. Dutta, and C.-C. Liu, "Smart sensor systems for spacecraft fire detection and air quality monitoring." *American Institute of Aeronautics and Astronautics*, **0**, 5021 (2011).
191. R. Spencer, "Certification considerations for the configuration of a hydrogen-fuelled aeroplane." *Aeronaut. J.*, **127**, 213 (2023).
192. J. Kopasz and T. Krause, *H2@ Airports Workshop Summary Report* (Argonne National Lab. (ANL), Argonne, IL (United States)) (2021).
193. marketsandmarkets.com. Gas Sensors Market by Gas Type (Oxygen, Carbon Monoxide, Carbon Dioxide, Nitrogen Oxide, Volatile Organic Compounds, Hydrocarbons), Technology, Output Type, Product Type, Application and Region - Global Forecast to 2027.
194. J. R. Stetter, "Introduction: experimental methods in chemical sensor and sensor array evaluation and development." *Computational Methods for Sensor Material Selection* (Springer US, New York, NY)3 (2009).
195. T. Wischmeyer, J. R. Stetter, W. J. Buttner, V. Patel, and D. Peaslee, "Characterization of a selective, zero power sensor for distributed sensing of hydrogen in energy applications." *Int. J. Hydrog. Energy*, **46**, 31489 (2021).
196. M. T. Carter, J. R. Stetter, M. W. Findlay, and V. Patel, "Amperometric gas sensors with ionic liquid electrolytes." *ECS Trans.*, **58**, 7 (2014).
197. M. T. Carter, J. R. Stetter, M. W. Findlay, and V. Patel, "Rational design of amperometric gas sensors with ionic liquid electrolytes." *ECS Trans.*, **64**, 95 (2014).
198. J. R. Stetter, S. Zaromb, W. R. Penrose, T. Otagawa, and A. F. Cohen, "Investigations into the feasibility of low-current methane sensors." *Anal. Chem. Symp. Ser.*, **17**, 214 (1983).
199. AlphaSense, Data Sheet AlphaSense H2-AF Hydrogen Sensor. https://www.alphasense.com/wp-content/uploads/2022/09/Alphasense_H2-AF_datasheet.pdf (accessed 2023-11-08).
200. Control Instruments Corporation, Data Sheet Control Instruments Corporation - Hydrogen Sensor for SmartMaxII. https://www.controlinstruments.com/sites/default/files/attached-pdf/Hydrogen_Specifications.pdf (accessed 2023-11-08).
201. Critical Environment, Specifications Critical Environment - Electrochemical Sensor. https://www.critical-environment.com/products/gas-detectors/cgas-detector-digital (accessed 2023-11-08).
202. Det-Tronics, Data Sheet Det-Tronics - Electrochemical Toxic Gas Detector. https://www.det-tronics.com/Content/Documents/90-1199-10.3_(GT3000).pdf (accessed 2023-11-08).
203. A. G. Drägerwerk, Data Sheet Drägerwerk AG - Electrochemical Sensor. https://www.draeger.com/Products/Content/sensor-ec-pi-9107421-en-us.pdf (accessed 2023-11-08).
204. Euro-Gas Management Services Ltd Data Sheet Euro-Gas Management Services Ltf. - 4-H2-40000 Hydrogen Sensor. https://euro-gasman.com/media/wysiwyg/Gas_Sensors/SOLIDSENSE/4_H2_40000.pdf (accessed 2023-11-08).
205. Teledyne Gas & Flame Detection, Data Sheet Teledyne Gas & Flame Detection - Model 100 Toxic Gas Sensor. https://www.teledynegasandflamedetection.com/sites/teledynegasandflamedetection.com/files/product-specs/GF30191D-EN_Model100_4pLetterBro.pdf (accessed 2023-11-08).
206. Teledyne Gas & Flame Detection, Data Sheet Teledyne Gas & Flame Detection - DGi-TT7-E Electrochemical Toxic Gas Detector. https://www.teledynegasandflamedetection.com/sites/teledynegasandflamedetection.com/files/product-specs/GF-00267E-EN-MultiTox_DGi-TT7-E_2pBroA4.pdf (accessed 2023-11-08).
207. Industrial Scientific, Data Sheet Industrial Scientific - IBRID MX6. https://fs.hubspotusercontent00.net/hubfs/4113657/_ISC2021/Supporting%20Documents/MXiBRID/MX6iBrid_SpecSheet_EN.pdf (accessed 2023-11-08).
208. Membrapor, Data Sheet Membrapor - Hydrogen Gas Sensor. https://www.membrapor.ch/sheet/Hydrogen-Gas-Sensor-H2-C-20000.pdf (accessed 2023-11-08).
209. International Gas Detectors, Data Sheet International Gas Detectors - SGT Single Gas Monitor. https://www.internationalgasdetectors.com/wp-content/uploads/2020/10/SGP-Single-Gas-Detector-V1.pdf (accessed 2023-11-08).
210. Safety Systems Technology, Data Sheet Safety Systems Technology - GT814 Nova-Sensor Elite. http://www.safetysys.com/wp-content/uploads/2015/03/GT814-toxic-gas-detector.pdf (accessed 2023-11-08).
211. Sensitron - A Halma Company, Data Sheet Sensitron - SMART3G-D2. https://www.sensitron.it/MT/P/DS/_DS4821%20SMART3GD2%20EC_EN.pdf (accessed 2023-11-08).
212. SGX Sensortech, Data Sheet SGX - EC4-1000-H2. https://www.sgxsensortech.com/content/uploads/2014/07/EC4-1000-H21.pdf (accessed 2023-11-08).
213. Zhengzhou Winsen Electronics Technology, User Manual Winsen Sensor - Model ZE03 https://www.winsen-sensor.com/d/files/ze03-electrochemical-module-manualv2_5.pdf (accessed 2023-11-08).
214. AlphaSense, Data Sheet AlphaSense - NH3-AF. https://www.alphasense.com/wp-content/uploads/2022/09/Alphasense_NH3-AF-2_datasheet.pdf (accessed 2023-11-08).
215. M. C. I. O. Ü. Evikon, Data Sheet Evikon MCI OÜ - Ammonia Detector-Transmitter E2608-NH3-E https://evikontroll.ee/pdf/evikon/E2608-NH3-E_DS_EN.pdf (accessed 2023-11-08).
216. Figaro Engineering Inc, Data Sheet Figaro Engineering Inc. - FECS44-100/-200. https://www.figaro.co.jp/en/product/docs/fecs44l_product%20infomation%28en%29_rev03.pdf (accessed 2023-11-08).
217. Teledyne Gas & Flame Detection, Data Sheet Teledyne Gas & Flame Detection - Model DM 700 https://www.teledynegasandflamedetection.com/sites/teledynegasandflamedetection.com/files/product-specs/GF-00239J-EN_DM-700_Letter_4pBro.pdf (accessed 2023-11-08).
218. Honeywell Analytics, Data Sheet Honeywell Analytics - EC-FX-NH3. https://prod-edam.honeywell.com/content/dam/honeywell-edam/sps/his/en-ca/products/gas-and-flame-detection/documents/bro1162en_ecfxnh3_brochure_v3_0116.pdf (accessed 2023-11-08).
219. LogiDataTech, Data Sheet LogiDataTech - MF420-C. https://logidata.tech/de/produkte/messfuehler/toxisch/mf420-c (accessed 2023-11-08).
220. Membrapor, Data Sheet Membrapor - Ammonia Gas Sensor. https://www.membrapor.ch/sheet/Ammonia-Gas-Sensor-NH3-CR-10000.pdf (accessed 2023-11-08).
221. Nemoto Sensor Engineering, Data Sheet Nemoto Sensor Engineering - NE4-NH3. https://sensor.nemoto.co.jp/en/product/detail/ne4-nh3/ (accessed 2023-11-08).
222. Process Sensing Technology, Data Sheet Process Sensing Technology - FGD10 Series https://www.processsensing.com/docs/datasheet/020_7-FGD10A-Technical-Data-Sheet.pdf (accessed 2023-11-08).

223. SGX Sensortech, Data Sheet SGX - SGX-4NH3-1000 https://www.sgxsensortech.com/content/uploads/2020/04/DS-0307-SGX-4NH3-1000-datasheetv2.pdf (accessed 2023-11-08).
224. M. V. Nikolic, V. Milovanovic, Z. Z. Vasiljevic, and Z. Stamenkovic, "Semiconductor gas sensors: materials, technology, design, and application." *Sensors*, **20**, 6694 (2020).
225. J. Kong, M. G. Chapline, and H. Dai, "Functionalized carbon nanotubes for molecular hydrogen sensors." *Adv. Mater.*, **13**, 1384 (2001).
226. D. Punetha, M. Kar, and S. K. Pandey, "A new type low-cost, flexible and wearable tertiary nanocomposite sensor for room temperature hydrogen gas sensing." *Sci Rep.*, **10**, 2151 (2020).
227. T. Seiyama, A. Kato, K. Fujiishi, and M. Nagatani, "A new detector for gaseous components using semiconductive thin films." *Anal. Chem.*, **34**, 1502 (1962).
228. K. Izawa, H. Ulmer, A. Staerz, U. Weimar, and N. Barsan, "Application of SMOX-Based sensors." *Gas Sensors Based on Conducting Metal Oxides*, ed. N. Barsan and K. Schierbaum (Elsevier Inc., United States) 217 (2018).
229. N. Barsan, "Transduction in semiconducting metal oxide based gas sensors - implications of the conduction mechanism." *Procedia Eng.*, **25**, 100 (2011).
230. N. Barsan and U. Weimar, "Conduction model of metal oxide gas sensors." *J. Electroceramics*, **7**, 143 (2001).
231. N. Barsan, D. Koziej, and U. Weimar, "Metal oxide-based gas sensor research: how to?" *Sens. Actuators B Chem.*, **121**, 18 (2007).
232. D. Degler, U. Weimar, and N. Barsan, "Current understanding of the fundamental mechanisms of doped and loaded semiconducting metal-oxide-based gas sensing materials." *ACS Sens.*, **4**, 2228 (2019).
233. D. R. Miller, S. A. Akbar, and P. A. Morris, "Nanoscale metal oxide-based heterojunctions for gas sensing: a review." *Sens. Actuators B Chem.*, **204**, 250 (2014).
234. T. Russ, M. Zhang, T. Zhou, U. Weimar, T. Zhang, and N. Barsan, "Chapter 7 - fabrication of metal oxide heterostructures for the application in chemoresistive gas sensors." *Metal Oxide-Based Heterostructures - Fabrication and Applications*, ed. N. Kumar and B. Soucase (Elsevier, Amsterdam) 247 (2022).
235. ResearchAndMarkets.com. Global Semiconductor Gas Sensors Market Research Report 2022: Sensing Materials and Applications https://www.businesswire.com/news/home/20221222005244/en/Global-Semiconductor-Gas-Sensors-Market-Research-Report-2022-Sensing-Materials-and-Applications—Copper-Oxide-Nanomaterial-Based-Gas-Sensors-Gaining-Wider-Adoption—ResearchAndMarkets.com (accessed 2023-11-08).
236. ScioSense, Data Sheet ScioSense - ENS160. https://www.sciosense.com/wp-content/uploads/documents/SC-001224-DS-9-ENS160-Datasheet.pdf (accessed 2023-11-08).
237. Duoyi Instruments, Data Sheet Duoyi Instrument - DY8800B. https://www.dyinstrument.com/products/pdf/catalog/DY8800B,DY5750B.pdf (accessed 2023-11-08).
238. Envin Scientific Limited, Data Sheet Envin Scientific Limited - SGHA-P2. https://www.envinsci.co.uk/wp-content/uploads/2016/04/Sensor-Gas-Chromatograph.pdf (accessed 2023-11-08).
239. M. C. I. O. Ü. Evikon, Data Sheet Evikon - E2608-LEL. https://evikontroll.ee/pdf/evikon/E2608-LEL_DS_EN.pdf (accessed 2023-11-08).
240. Nissha FIS Inc, Data Sheet Nissha FIS, Inc. - SB-19-00. https://www.fisinc.co.jp/en/common/pdf/SB1900E.pdf (accessed 2023-11-08).
241. SGX Sensortech, Data Sheet SGX - MiCS-5914. https://www.sgxsensortech.com/content/uploads/2014/07/1108_Datasheet-MiCS-5914.pdf (accessed 2023-11-08).
242. M. C. I. O. Ü. Evikon, Data Sheet Evikon OÜ - E2608-CH4. https://evikontroll.ee/pdf/evikon/E2608-CH4_DS_EN.pdf (accessed 2023-11-08).
243. Figaro Engineering Inc, Data Sheet Figaro Engineering Inc. - TGS 2611-C00. https://www.figaro.co.jp/en/product/docs/tgs2611-c00_product%20information%28en%29rev01.pdf (accessed 2023-11-08).
244. F. I. S. Nissha, Inc. Data Sheet Nissha FIS, Inc. - SB-95-12. https://www.fisinc.co.jp/en/common/pdf/SB9512E.pdf (accessed 2023-11-08).
245. LogiDataTech, Data Sheet LogiDataTech - MF420-H. https://logidata.tech/de/produkte/messfuehler/explosiv/mf420-h (accessed 2023-11-08).
246. Zhengzhou Winsen Electronics Technology, Data Sheet Winsen Electronics - MQ-4 https://www.winsen-sensor.com/d/files/mq-4-(ver1_6)—manual.pdf (accessed 2023-11-08).
247. SGX Sensortech, Data Sheet SGX - MiCS-5524 https://www.sgxsensortech.com/content/uploads/2014/07/1084_Datasheet-MiCS-5524-rev-8.pdf (accessed 2023-11-08).
248. P. Atkins and J. de Paula, *Atkins' Physical Chemistry* 10th Ed. P. Atkins and J. de Paula, (Oxford University Press, Oxford) 1008 (2014).
249. Y. Zhang, H. Peng, X. Qian, Y. Zhang, G. An, and Y. Zhao, "Recent advancements in optical fiber hydrogen sensors." *Sens. Actuators B Chem.*, **244**, 393 (2017).
250. G. Wang, J. Dai, and M. Yang, "Fiber-optic hydrogen sensors: a review." *IEEE Sens. J.*, **21**, 12706 (2021).
251. J. Dai, L. Zhu, G. Wang, F. Xiang, Y. Qin, M. Wang, and M. Yang, "Optical fiber grating hydrogen sensors: a review." *Sensors*, **17**, 577 (2017).
252. A. K. Pathak, S. Verma, N. Sakda, C. Viphavakit, R. Chitaree, and B. M. A. Rahman, "Recent advances in optical hydrogen sensor including use of metal and metal alloys: a review." *Photonics*, **10**, 122 (2023).
253. K. Chen, D. Yuan, and Y. Zhao, "Review of optical hydrogen sensors based on metal hydrides: recent developments and challenges." *Opt. Laser Technol.*, **137**, 106808 (2021).
254. marketsandmarkets.com. Non-Dispersive Infrared (NDIR) Market by Gas Type (Carbon Dioxide, Hydrocarbons, Others), Application (Monitoring, HVAC, Detection and Analysis), Vertical (Industrial & Manufacturing, Oil & Gas) and Region - Global Forecast to 2027 https://www.marketsandmarkets.com/Market-Reports/non-dispersive-infrared-market-90187624.html (accessed 2023-11-08).
255. R. Bogue, "Detecting gases with light: a review of optical gas sensor technologies." *Sens. Rev.*, **35**, 133 (2015).
256. Materion GmbH, Data sheet materion gmbh - MOHS (accessed 2023-11-08) (2023), https://materion-gmbh.de/download/Visio-dataMOHS2_2.pdf.
257. Alphasense, Data sheet alphasense - irm-at. 9 (accessed 2023-11-08) (2023), https://alphasense.com/wp-content/uploads/2022/09/Alphasense_IRM-AT_datasheet.pdf.
258. A. G. Drägerwerk, Data Sheet Drägerwerk AG - MetCam. https://www.draeger.com/Products/Content/metcam-gascamera-pi-9107419-en-us.pdf (accessed 2023-11-08).
259. Teledyne Gas & Flame Detection, Data Sheet Teledyne Gas & Flame Detection - GD10 P. https://www.teledynegasandflamedetection.com/en-us/Products/docs/fixedgas-gd10series-gd10p-usermanual-english.pdf (accessed 2023-11-08).
260. Teledyne Gas & Flame Detection, Data Sheet Teledyne Gas & Flame Detection - GD10PE. https://www.teledynegasandflamedetection.com/sites/teledynegasandflamedetection.com/files/GF-00269L-EN-GD10PE_2pBroA4.pdf (accessed 2023-11-08).
261. Teledyne Gas & Flame Detection, Data Sheet Teledyne Gas & Flame Detection - SafEye Quasar 900 https://www.teledynegasandflamedetection.com/sites/teledynegasandflamedetection.com/files/GF30166E-EN_Spyglass_4pBroA4.pdf (accessed 2023-11-08).
262. Honeywell Analytics, Data Sheet Honeywell - Searchpoint Optima Plus. https://prod-edam.honeywell.com/content/dam/honeywell-edam/sps/his/en-ca/products/gas-and-flame-detection/documents/11257spoint_optimads0276v11_06_15.pdf (accessed 2023-11-08).
263. MSA - The Safety Company. Data Sheet MSA - Senscient ELDS. https://us.msasafety.com/Fixed-Gas-&-Flame-Detection/Gas-Detectors/Senscient-ELDS%e2%84%a2-Open-Path-Gas-Detector/p/000140001100001000?utm_medium=301&utm_source=senscient.com (accessed 2023-11-08).
264. Nova - Dependable Gas Analysis Solutions, Data Sheet Nova - 470 Flexi-Nova Series. https://catalog.nova-gas.com/Asset/470%20FlexiNova%20Hydrocarbons%20Analyzer21.pdf (accessed 2023-11-08).
265. Fer Strumenti, Data Sheet Fer Strumenti - ENOX II. https://www.fer-strumenti.com/wp-content/uploads/2019/01/analizzatore-gas-enox-ii-EN.pdf (accessed 2023-11-08).
266. SGX Sensortech, Data Sheet SGX - IR1 Single Gas Series. https://www.sgxsensortech.com/content/uploads/2014/07/DS-0247-IR1-Single-Gas-Series-Datasheet-V2.pdf (accessed 2023-11-08).
267. ION Science Ltd Data Sheet ION Science - VOC Gas Sensor. https://ionscience.com/en/products/minipid-2-ppm-gas-sensor/#technical-specification (accessed 2023-11-08).
268. SPECTREX, Data Sheet SPECTREX - SafEye Quasar 960. https://www.gdscorp.com/site/wp-content/uploads/2022/04/product-data-sheet-safeye-quasar-960-en-us-7027748.pdf (accessed 2023-11-08).
269. Honeywell Analytics, Data Sheet Honeywell - RAEGuard 2 PID. https://prod-edam.honeywell.com/content/dam/honeywell-edam/sps/his/en-ca/products/gas-and-flame-detection/documents/HIS_Gas_RAEGuard20220PID_DS_EMEA_0419_FINAL.pdf (accessed 2023-11-08).
270. AZoSensors.com. Infrared vs Catalytic Bead Gas Detectors: Usage in Combustible Gas Safety Monitoring https://www.azosensors.com/article.aspx?ArticleID=2135#:~:text=Catalytic%20Bead%20Sensing&text=Being%20single%2Dpoint%20combustible%20gas,Wheatstone%20Bridge%2Dtype%20temperature%20transducer. (accessed 2023-11-08).
271. D. Struk, A. Shirke, A. Mahdavifar, P. J. Hesketh, and J. R. Stetter, "Investigating time-resolved response of micro thermal conductivity sensor under various modes of operation." *Sens. Actuators B Chem.*, **254**, 771 (2018).
272. A. Mahdavifar, M. Navaei, P. J. Hesketh, M. Findlay, J. R. Stetter, and G. W. Hunter, "Transient thermal response of micro-thermal conductivity detector (μTCD) for the identification of gas mixtures: An ultra-fast and low power method." *Microsyst. Nanoeng.*, **1**, 15025 (2015).
273. ADEV S.r.L, Data Sheet Adev - 8867 https://www.htk-hamburg.com/media/factsheets/XXXX67_Datasheet-engl.pdf (accessed 2023-11-08).
274. AirTest Technologies Inc, Data Sheet AirTest - TR5200. https://assets.kele.com/product-assets/air-test-techonologies/skus/tr5200-h2/related/install-sheet_2846_tr5200-h2.pdf (accessed 2023-11-08).
275. Analox Group, Data Sheet Analox - DAMS. https://drive.google.com/file/d/1sHknpToU4weJ2SvQ2-DFgN6pzR34NS3v/view (accessed 2023-11-08).
276. Crowcon Detection Instruments, Data Sheet Crowcon - Gasman. https://www.crowcon.com/wp-content/uploads/2018/12/Gasman-Datasheet-US-English-Letter-Size.pdf (accessed 2023-11-08).
277. Det-Tronics, Data Sheet Det-Tronics - Model CGS. https://www.det-tronics.com/content/documents/90-1041-9.2-(CGS-Specifications).pdf (accessed 2023-11-08).
278. A. G. Drägerwerk, Data Sheet Drägerwerk AG - Polytron 8200 CAT. https://www.draeger.com/Products/Content/polytron-8200-pi-9107415-en-us.pdf (accessed 2023-11-08).
279. Evikon MCI OÜ, Data Sheet Evikon OÜ - E2608-LEL. https://evikontroll.ee/pdf/evikon/E2608-LEL_DS_EN.pdf (accessed 2023-11-08).
280. Figaro Engineering Inc, Data Sheet Figaro - TGS6812-D00. https://www.figaro.co.jp/en/product/docs/tgs6812-d00_product_information%28en%29_rev05.pdf (accessed 2023-11-08).
281. General Tools, Data sheet general tools - combustible gas leak detector. (accessed 2023-11-08) (2023), https://generaltools.com/combustible-gas-leak-detector.

282. Kane International Ltd Data Sheet Kane - Combustible Gas Leak Detector. (2023), https://kane.co.uk/products/KANE-EGD.
283. MSA - The Safety Company, Data Sheet MSA - ALTAIR Io (accessed 2023-11-08) (2023), https://us.msasafety.com/Portable-Gas-Detection/Multi-Gas/ALTAIR-io%E2%84%A2-4-Gas-Detection-Wearable/p/000170000800001001?section=resources.
284. City Technology Engineering Safety, Data Sheet City Technology - MICROpel 75M. https://prod-edam.honeywell.com/content/dam/honeywell-edam/sps/siot/en-ca/products/sensors/gas-sensors/microcel/documents/sps-siot-citytech-micropel-75m-sensor-datasheet.pdf (accessed 2023-11-08).
285. LogiDataTech. Data Sheet LogiDataTech - MF420-P. https://logidata.tech/de/produkte/messfuehler/explosiv/mf420-p (accessed 2023-11-08).
286. Kebaili. Data Sheet Kebaili - KHS-200. https://www.kebaili.com/pd-khs-200-hydrogen-sensor.cfm (accessed 2023-11-08).
287. Nemoto Sensor Engineering. Data Sheet Nemoto - NAP-100AH-P. https://sensor.nemoto.co.jp/en/product/detail/nap-100ah-p/ (accessed 2023-11-08).
288. *Posifa Technologies Inc., MEMS THERMAL CONDUCTIVITY HYDROGEN SENSORS, Datasheet_PGS1000_MEMS_TC_H2_RevA_C0.5.Pdf*; 2020 https://posifatech.com/wp-content/uploads/2020/11/Datasheet_PGS1000_MEMS_TC_H2_RevA_C0.5.pdf (accessed 2023-11-08).
289. SGX Sensortech. Data Sheet SGX - TCD. https://www.sgxsensortech.com/content/uploads/2016/06/DS-0223-VQ500-Datasheet-V2.pdf (accessed 2023-11-08).
290. Xensor. Data Sheet Xensor - XEN-5320-HP. https://xensor.nl/images/pdf-files/XEN-5320-HP-USB.pdf (accessed 2023-11-08).
291. Teledyne Gas & Flame Detection. Data Sheet Teledyne Gas & Flame Detection - DG-TX7 https://www.teledynegasandflamedetection.com/sites/teledynegasandflamedetection.com/files/product-specs/GF-30083E-EN-MultiXplo_DG-TX7_2pBroA4.pdf (accessed 2023-11-08).
292. Safety Systems Technology. Data Sheet Safety Systems - GC804 http://www.safetysys.com/wp-content/uploads/2015/02/GC804-combustible-gas-detector.pdf (accessed 2023-11-08).
293. W. H. King Jr, "Piezoelectric sorption detector." *Anal. Chem.*, **36**, 1735 (1964).
294. S. S. Ba Hashwan et al., "A review of piezoelectric MEMS sensors and actuators for gas detection application." *Discov. Nano*, **18**, 25 (2023).
295. N. Miura, H. Minamoto, G. Sakai, and N. Yamazoe, "New-type calorimetric gas sensor using temperature characteristics of piezoelectric quartz crystal fitted with noble metal catalyst film." *Sens. Actuators B*, **5**, 211 (1991).
296. S. Dong, F. Bai, J. F. Li, and D. Viehland, "Sound-resonance hydrogen sensor." *Appl. Phys. Lett.*, **82**, 4590 (2003).
297. A. C. Fechete, W. Wlodarski, K. Kalantar-Zadeh, A. S. Holland, J. Antoszewski, S. Kaciulis, and L. Pandolfi, "SAW-Based gas sensors with Rf sputtered InOx and PECVD SiNx films: response to H2 and O3 gases." *Sens. Actuators B Chem.*, **118**, 362 (2006).
298. J. Wan, M. Ioffe, and M. Depew, "A novel acoustic sensing system for on-line hydrogen measurements." *Sens. Actuators B*, **32**, 233 (1996).
299. J. C. Vyas, V. R. Katti, S. K. Gupta, and J. V. Yakhmi, "A non-invasive ultrasonic gas sensor for binary gas mixtures." *Sens. Actuators B Chem.*, **115**, 28 (2006).
300. Wood. Speed of Sound in Gases - List. https://www.betamachinery.com/knowledge-center/speed-of-sound-in-gases-list (2023).
301. ATO. Data Sheet ATO - Portable H2 Detector. https://www.ato.com/Content/doc/ATO-SKY2000-gas-detector-user-manual.pdf (2023).
302. Industrial Safety. Data Sheet Industrial Safety - H2 https://www.grainger.com/product/52HP32?gucid=N:N:PS:Paid:GGL:CSM-2295:4P7A1P:20501231&gclid=CjwKCAiA3KefBhByEiwAi2LDHMaUD_tLzLfn7PtHZw4mdKiZpQNwV5-zpkRg8SnOYqfzYiKUAU6jWBoC5vEQAvD_BwE&gclsrc=aw.ds (2023).
303. Analytical Technology Inc. Data Sheet ATi - H2 PortaSens https://gas-sensing.com/downloads/ati/d16/d16-portasensIII-information-sheet.pdf (2023).
304. Industrial Safety, Data Sheet Indutrial Safety - NH3 https://grainger.com/product/8YET0?gucid=N:N:PS:Paid:GGL:CSM-2295:4P7A1P:20501231&gclid=CjwKCAiA3KefBhByEiwAi2LDHPS5sfyGTm0DNLEyeBNkXE8cH_bFKplWfCW-M8u96bjqYLgzj3HubIBoCgpQQAvD_BwE&gclsrc=aw.ds (2023).
305. BW Technologies, Data Sheet BW Technologies - NH3 https://grainger.com/product/4KEF7?gucid=N:N:PS:Paid:GGL:CSM-2296:9JMEDM:20500731&gclid=CjwKCAiA3KefBhByEiwAi2LDHNLaH4B22ErfHIlLp6Az6BRTLGA7M4WN0S-VGHrcdRo6V02Ailz4V3xoCb4cQAvD_BwE&gclsrc=aw.ds (2023).
306. Macurco. Data Sheet Macurco - C3H8, CH4, H2. https://grainger.com/product/45CJ95?gucid=N:N:PS:Paid:GGL:CSM-2295:4P7A1P:20501231&gclid=CjwKCAiA3KefBhByEiwAi2LDHPngrWAYJbmwtiLyM_4jv5NEyBqtbhhB-VlBt24UrVLBZh2ztB-VgBoCUXwQAvD_BwE&gclsrc=aw.ds (2023).
307. R. R. Rye and A. J. Ricco, "Ultrahigh vacuum studies of Pd metal-insulator-semiconductor diode H2 sensors." *J. Appl. Phys.*, **62**, 1084 (1987).
308. H2Scan. Data Sheet H2Scan - HY OPTIMA 2700 Series. https://h2scan.com/wp-content/uploads/2020/09/90000133-r3-hy-optima-2700-technical-data-sheet.pdf (2023).
309. Det-Tronics. data sheet det-tronics - flexsonic acoustic. https://det-tronics.com/content/documents/90-1208-2.1-(FlexSonic-Acoustic).pdf (2023).
310. Riken Keiki co ltd riken keiki co. ltd - ocd-800 (2023), https://product.rikenkeiki.co.jp/lp/en/ohc-800/?gclid=Cj0KCQiA54KfBhCKARIsAJzSrdr_g-2lSu83pBXF1yZay4akWTDXtY4a-eZZ8Hn9B08joAqtSV14FxIaArxJEALw_wcB.
311. S. S. Das, G. Kopnov, and A. Gerber, "Detection of hydrogen by the extraordinary hall effect in CoPd alloys." *J. Appl. Phys.*, **124**, 104502 (2018).
312. W. C. Lin, C. J. Tsai, H.-Y. Huang, B.-Y. Wang, V. R. Mudinepalli, and H.-C. Chiu, "Hydrogen-mediated long-range magnetic ordering in Pd-Rich alloy film." *Appl. Phys. Lett.*, **106**, 012404 (2015).
313. H2Scan. Data Sheet H2Scan - HY-ALERTA (2023), https://h2scan.com/wp-content/uploads/2020/10/h2scan-safety-products-data-sheet-90000009r3.pdf.
314. *Incus Ultrasonic Gas Leak Detector for Wide Area Gas Leaks | Emerson US.* https://emerson.com/en-us/catalog/rosemount-sku-incus-ultrasonic-gas-leak-detector?fetchFacets=true#facet:&partsFacet:&modelsFacet:&facetLimit:&searchTerm:&partsSearchTerm:&modelsSearchTerm:&productBeginIndex:0&partsBeginIndex:0&modelsBeginIndex:0&orderBy:&partsOrderBy:&modelsOrderBy:&pageView:list&minPrice:&maxPrice:&pageSize:&facetRange:& (accessed 2023-09-11).
315. *Dräger Polytron® 6100 EC WL | Draeger* https://draeger.com/en-us_us/Products/Polytron-6100-EC-WL (accessed 2023-09-11) (2023).